Charge transport through molecular switches

2010 J. Phys.: Condens. Matter 22 133001

(http://iopscience.iop.org/0953-8984/22/13/133001)

J. Phys.: Condens. Matter **22** (2010) 133001 (30pp) doi:10.1088/0953-8984/22/13/133001

TOPICAL REVIEW

Charge transport through molecular switches

Sense Jan van der Molen[1,3] **and Peter Liljeroth**[2]

[1] Kamerlingh Onnes Laboratorium, Leiden University, Niels Bohrweg 2, 2333 CA Leiden, The Netherlands
[2] Condensed Matter and Interfaces, Debye Institute for Nanomaterials Science, University of Utrecht, PO Box 80000, 3508 TA Utrecht, The Netherlands

E-mail: molen@physics.leidenuniv.nl

Received 26 November 2009, in final form 21 January 2010
Published 17 March 2010
Online at stacks.iop.org/JPhysCM/22/133001

Abstract
We review the fascinating research on charge transport through switchable molecules. In the past decade, detailed investigations have been performed on a great variety of molecular switches, including mechanically interlocked switches (rotaxanes and catenanes), redox-active molecules and photochromic switches (e.g. azobenzenes and diarylethenes). To probe these molecules, both individually and in self-assembled monolayers (SAMs), a broad set of methods have been developed. These range from low temperature scanning tunneling microscopy (STM) via two-terminal break junctions to larger scale SAM-based devices. It is generally found that the electronic coupling between molecules and electrodes has a profound influence on the properties of such molecular junctions. For example, an intrinsically switchable molecule may lose its functionality after it is contacted. Vice versa, switchable two-terminal devices may be created using passive molecules ('extrinsic switching'). Developing a detailed understanding of the relation between coupling and switchability will be of key importance for both future research and technology.

(Some figures in this article are in colour only in the electronic version)

Contents

[3] Author to whom any correspondence should be addressed.

1. Introduction

Molecular electronics is based on an idea that is as simple as it is captivating: by combining the expertise of chemistry and physics, one should be able to create 'custom-designed' molecular devices. Obviously, this process requires two steps. First, the desired function should be encoded in a single molecule. Then, the molecule should be connected to electrodes. Already in 1971, Mann and Kuhn demonstrated the feasibility of hybrid metal–molecule devices [1]. However, they focused on passive molecules only. It was not until the seminal 1974 contribution of Aviram and Ratner that the great potential of molecular electronics was truly realized [2, 3].

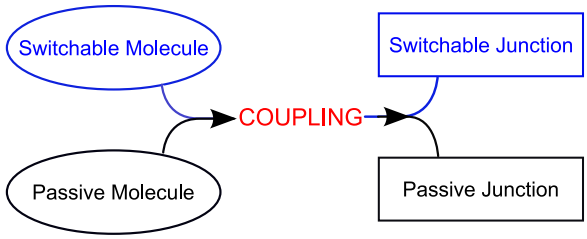

Figure 1. Schematic picture of how coupling can influence the performance of a molecular device. Naively, one may expect a switchable molecule to keep functioning after it is connected to one or two metal electrodes. We will call this *intrinsic* switching. However, if the electronic coupling between metal and molecule becomes too strong, a switchable molecule may lose its functionality and become passive. Remarkably, the opposite is possible too. A molecular device containing a passive molecule may turn out to have switchable properties. Such *extrinsic* switching may be the result of various phenomena related to the exact interaction between molecule and electrodes, applied voltage bias, current and local electric field.

They presented a theoretical description of a single molecular diode, based on a carefully designed asymmetric molecule. It is fair to say that, with these two pioneering contributions, the area of molecular charge transport took off. By the end of the last millennium, it had become a major subfield of nanoscience. This was not only a result of the promise of designable nanodevices. The research is also of fundamental interest, as molecular charge transport is quantum mechanical in nature at any temperature. Moreover, molecules form beautiful systems to study electron–electron interaction (Coulomb blockade), spin–spin interaction (Kondo effects) and electron-vibration (electron–phonon) interaction.

Arguably, the most appealing example of a functional molecule is formed by a molecular switch, i.e. a molecule in which the electronic communication can be controlled externally [4–7]. Devices based on switchable molecules could, in principle, function as memory elements with very advantageous properties with respect to size (∼nanometers), speed (potential switching times ∼100 ps) and stability (large energy barrier between the two molecular states). However, it is only during the past 15 years that serious attempts have been made to connect such molecules to electrodes so as to fundamentally study their charge transport properties. Interestingly, these research efforts have led to as many results as surprises. This has everything to do with the fact that it is impossible to connect a molecule to a metal without influencing its properties. Depending on the strength of the electronic coupling, this may or may not lead to functionality loss of the molecule. In other words, a molecule that is switchable in solution may become passive in a device. Remarkably, the reverse phenomenon exists as well. A device may exhibit switchable properties even when a non-switchable (passive) molecule is at its core. At the moment, our understanding of this phenomenon, which we will call *extrinsic* switching, is limited. This is mostly due to the lack of atomic level understanding and control over the molecule–metal contacts. The richness of the field of switchable molecular devices is perhaps best illustrated by figure 1.

Inspired by the fascinating science performed within our community, we believe that a review on molecular devices based on switchable molecules is due. Our main focus will be on intrinsic switching, i.e. switching of junctions incorporating a bistable molecule. However, extrinsic switching will be given its share of attention as well. As to the experimental techniques, we do not limit ourselves to two-terminal metal–molecule–metal junctions. Much of the interesting science has been the product of scanning tunneling microscopy (STM) studies of molecules on surfaces. We feel that these techniques are complementary and their combination is essential for a more detailed understanding of the phenomena relevant to this challenging field.

2. Switchable molecules

The design and synthesis of bistable switchable molecules is undoubtedly one of the great triumphs in the nascent field of molecular electronics. Generally, the design of an original type of switch consists of two steps. First, the proof of principle of the operation of a novel switch has to be demonstrated. Next, its properties are optimized by subtly changing the molecular structure. This generally leads to 'families' of molecules based on the same switching principle. Clearly, for charge transport measurements, a third step is necessary, i.e. contacting the molecule to electrodes. If the metal–molecule coupling leads to a loss of functionality (see figure 1), another optimization cycle in synthesis may become necessary. From such research, a fundamental understanding of the full system may be obtained.

Over the years, a wide variety of molecular switches have been described in the literature. Moreover, a broad spectrum of stimuli can be used to activate ('switch') these molecules. The switching mechanisms can be coarsely divided into conformational and charging/redox switches. In the first case, an isomerization reaction takes place which fundamentally changes the three-dimensional structure of the molecule. In the second case, a molecule takes up (or gives up) an electron, leading to a different charge state. Of course, minor conformational changes due to a change in the molecular redox state (reorganization) are inevitable. Nevertheless, we choose the distinction above, since pure conformational switches do not involve a change of the molecular charge. Below, we introduce the mechanisms responsible for the operation of molecular switches and stimuli that have drawn most attention in molecular transport research.

2.1. Intrinsic molecular switches

In general, molecular switchability requires the existence of two isomers, which can be controllably converted into one another by some external stimulus. In our specific case, we have an additional requirement: both isomers need to give rise to significantly different conductance properties. To introduce the basics of molecular switching, we refer to figure 2. Here, we show a generalized diagram of the potential energy surfaces of a switchable molecule. The 'reaction coordinate' on the x axis is usually a physical quantity that describes the passage

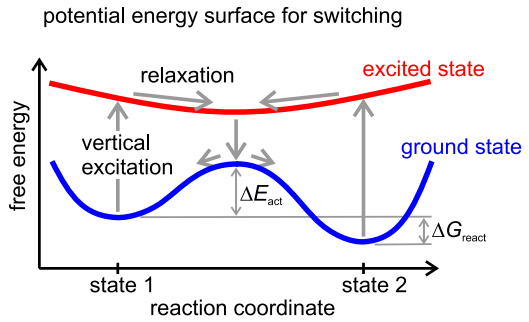

Figure 2. Typical potential energy surface of a two-state molecular switch. On the x axis, a 'reaction coordinate' is shown. This is generally a physical parameter such as a distance between two atoms or an angle between two rings within the molecule. The ground state exhibits two local minima, which correspond to the two states of the switch. Switching can be achieved by bringing the molecule to an excited state, e.g. by illumination. The subsequent relaxation path can lead to a change of state with some probability. Alternatively, switching may be induced by exciting the molecule over the ground state barrier. This may be achieved by heating, excitation of vibrations by electrons, or by a high local electric field. We note that, depending on the switchable molecule considered, the excited state potential energy surface may have a more complicated shape, e.g. containing additional minima.

of the system from the reactants to products. This can be a distance between two atoms within the molecule or an internal torsion angle, e.g. between two benzene rings. The two states of the switch can be recognized by the two minima in the ground state potential energy surface. Generally, only one of the isomers is stable; the other state is metastable with a free energy that is higher by $\Delta G_{\mathrm{react}}$. A necessary condition for a useful bistable molecule is that the energy barrier between both states, ΔE_{act}, is much larger than the thermal energy $k_{\mathrm{B}}T$. To switch the molecule, one obviously needs to overcome this barrier. This can be done in two ways. First, one can bring the molecule to an excited state, e.g. by illumination. As a result, the molecule may relax over the excited potential energy surface (the upper curve in figure 2) and get converted into the other form. Clearly, this is a probabilistic process: in a certain percentage of cases, the conversion will not succeed. Interestingly, the probabilities may change dramatically after a molecule is connected to a metal. Alternatively, one may switch a molecule by driving it over the ground state barrier directly. This may be achieved by various means. First, continuous excitation of molecular vibrations by transported electrons may induce switching ('current-induced' switching by inelastic scattering). Second, a sufficiently high electric field acting on a molecule could induce the conversion ('field-induced' switching). Finally, heating of the molecular system may result in (non-selective) switching.

2.1.1. Conformational switches. Above, we defined a conformational switch as a switchable molecule, which has isomers with a different three-dimensional structure. A further division can be made. First, a change may take place in the 3D molecular conformation, without a modification of the bond structure. This is called *stereoisomerization*. Second, isomerization may take place by a reshuffling of

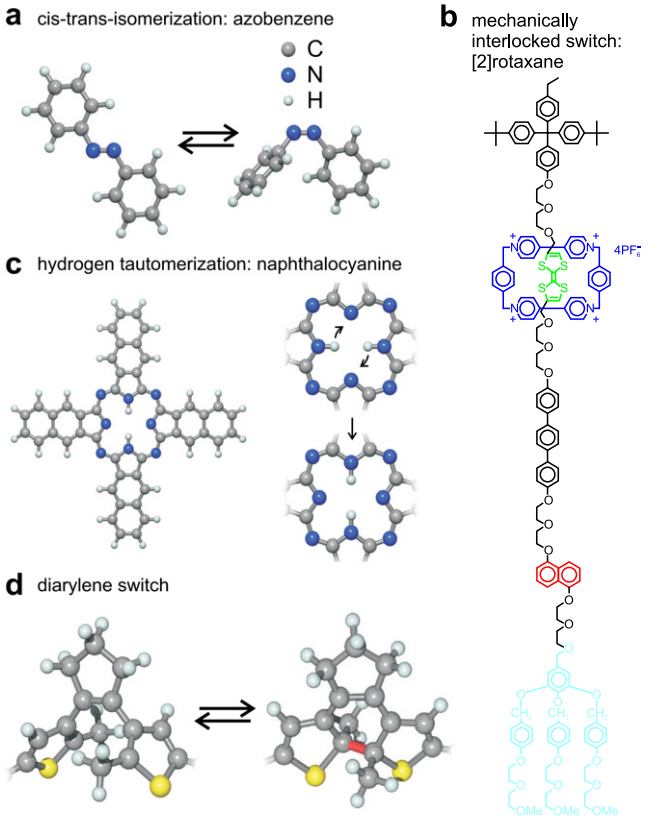

Figure 3. Examples of different switching mechanisms. (a) *Cis–trans* isomerization of azobenzene. (b) Example of a conformational switch consisting of two interlocked molecules. Switching is equivalent to movement of the ring (blue) between two stations (upper, green and lower, red) along the dumbbell molecule. (c) Switching based on a hydrogen tautomerization reaction: the position of the hydrogen atoms in the center of a naphthalocyanine molecule can be switched between left–right and top–bottom configurations, resulting in the rotation of all molecular orbitals by 90°. (d) Diarylethene switch. Switching between a cross-conjugated 'off' state (left) and a conjugated 'on' state (right) is possible by illumination by ultraviolet light ('off' to 'on') and visible light ('on' to 'off'), respectively. The C–C bond indicated in red in the 'on' (or 'closed') state is broken upon switching to the 'off' (or 'open') isomer.

the intramolecular chemical bonds. This is referred to as *structural isomerization*. The use of stereoisomerization in molecular switches has been demonstrated most notably by the well-known *cis–trans* (photo)isomerization in the family of azobenzene molecules [8–11]. In figure 3(a), both isomers of azobenzene are shown. A special group of switches exhibiting stereoisomerization is formed by the catenanes and rotaxanes (see figure 3(b)) [7]. These are mechanically interlocked molecules, basically consisting of two molecules 'embracing' each other. Generally, an outer ring can be reversibly moved between two stations of an inner molecule, giving rise to two different conductance values. Hence, one could consider this switching process *intermolecular stereoisomerization*, as in the first approximation only the position of one molecule with respect to the other changes[4].

[4] We note that, formally, a rotaxane (or catenane) unit is a single molecule, since one has to break a chemical bond to separate the subunits. If one takes this point of view, intramolecular stereoisomerization is the correct term to describe the switching process.

An elegant example of structural isomerization is the hydrogen tautomerization reaction in naphthalocyanine (see figure 3(c)) [12]. In this case, the two hydrogens in the central cavity of the molecule can change position in a sequential, two-step reaction: the intermediate conformation where the two H atoms occupy nearest-neighbor sites is not stable due to steric hindrance. Thus the movement of two small atoms leads to an effective 90° rotation of the molecular structure. Another example of structural isomerization is formed by the photoisomerization reaction of diarylethene molecules [5]. The two isomers of this type of molecule differ in their conjugation, but have very similar lengths (see figure 3(d)). The 'on'-state isomer is linearly conjugated over its full length, whereas the 'off'-state is cross-conjugated. Selective switching between both isomers is possible by using light with an appropriate wavelength.

We finish this section by noting that molecular switches should eventually be used in two-terminal devices or in molecular assemblies. Ideally, the switching process should therefore only modify the conductance of the molecule, not its overall physical size. Strictly speaking, this requirement is not met by any of the conformational switches. However, various molecular systems, including diarylethenes and naphthalocyanines, are close to satisfying this requirement.

2.1.2. Redox switches. Charge switching is intimately linked to reduction–oxidation (redox) reactions in electrochemistry and involves a permanent change of the number of electrons on the molecule. In an electrochemical set-up, the electrochemical potential of an electrode can be tuned with respect to the molecular energy levels. If the electrochemical potential is outside the HOMO–LUMO gap of the molecule, this naturally leads to charging of the molecule. If the molecule takes up an electron (the LUMO level becomes available), one speaks of reduction. Vice versa, if an electron is donated (or a hole is taken up, as the HOMO level becomes available), the process is called oxidation. In contrast to solution-based electrochemistry, permanent charging of the molecules in a two-terminal set-up requires some additional mechanism for stabilizing the different charge states. This involves a reorganization in the molecule and contacts that lowers the energy of the charged state below the Fermi level of the electrodes [13, 14]. In the absence of this stabilization mechanism, the added electron will simply tunnel out of the molecule.

Charge switching has been explored in molecules where a traditional redox couple has been synthesized with linker groups that allow the molecule to be covalently attached to electrodes. While it has been difficult to achieve and prove charge bistability as the switching mechanism in two-terminal experiments [15], a different form of charge switching has been studied in detail in three-terminal experiments. Using the gate electrode, the charge state of the molecule can be controlled while simultaneously recording the changes in the molecular conductance [16–20]. This differs from intrinsic molecular switching based on charge bistability in that there is no significant hysteresis: for any given gate potential, only one charge state is observed [21]. Nevertheless, three-terminal experiments yield extremely valuable information on the effect of the charge state on the molecular conductance.

2.2. Stimuli

Various external stimuli can, in principle, be applied to switch a molecular device. Indeed, switching may be current-induced, field-induced or light-induced. Furthermore, charge switching is possible by tuning the electrochemical potential. An intriguing indication of the versatility of molecular systems is the wide variety of stimuli that can be used to operate the very same molecule. For example, it has been demonstrated by STM experiments that the well-studied *cis–trans* isomerization of azobenzene can be induced by an applied electric field [8], inelastic tunneling [9] or illumination [10, 11]. Below, we introduce the various stimuli in more detail.

2.2.1. Current-induced switching. One of the ways to induce molecular switching is to make use of the electrons tunneling through the molecule. If their energy is sufficiently high, they are able to excite molecular vibrations (inelastic tunneling). For this mechanism to be operational, the applied bias V_b needs to be at least as high as the phonon energy $\hbar\omega$ involved, $eV_b \geqslant \hbar\omega$ [9, 22–24]. In many cases, the molecular energy barrier is larger than the phonon energy involved. In that case, a process is possible in which the barrier is 'climbed' by subsequent excitations into higher vibrational states of the molecule. This mechanism, named vibrational heating, is responsible for the famous Xe atom switch reported by Eigler *et al* [25].

2.2.2. Redox-potential-induced switching. Molecular charging may occur via virtual occupation of an ionization level or by resonant tunneling to a molecular orbital, followed by geometric reorganization that stabilizes the charge state [13, 26]. Alternatively, it may result from external gating that changes the energetic position of the molecular energy levels with respect to the Fermi level of the contacts, thus leading to charging [27]. Charging will generally result in significant changes in the molecular conductivity and can hence be used as a switching mechanism. In the case of charge switching, the absolute position of the molecular energy levels with respect to the Fermi energy of the electrodes and the polarizability of the environment are important [28]. They control the energetics of charging and the stability of the different charge states. In a typical experiment, an electrochemically gated set-up is used to control the electrochemical potential of a redox molecule with respect to a reference electrode in solution. For example, tuning the molecular energy levels (redox states) of an Fe(III)-protoporphyrin was demonstrated in an electrochemical STM set-up. This lead to a change of the molecular conductance by an order of magnitude [16].

An innovative proposal for a switchable molecular junction controlled by the electrochemical potential is due to Grunder *et al* [29]. We mention it here, because it is one of the few examples where the functionality of the anticipated device depends explicitly on the presence of the electrodes. It

could therefore be seen as an 'extrinsic' device *by design*. The authors synthesized a cruciform type of molecule, containing two rod-like substructures, one with sulfur anchor groups and one with pyridine endgroups. The basic idea for a future device is that the electrochemical potential controls the number of connections of the full gold–molecule–gold device. At negative potential, only one rod should span the junction (Au–S bonds). At positive potential both rods should couple to both electrodes, leading to a conductance increase.

For completeness, we note that the driving mechanism to switch mechanically interlocked molecules is also an oxidation (reduction) reaction, which charges (discharges) one of the stations of the inner molecule (green in figure 3(b)). Hence, rotaxanes and catenanes can be considered both conformational and redox switches. Because of their dominant conformational changes and also due to their large historical impact on the field, we will deal with experiments on these molecules in a separate section below.

2.2.3. Field-induced switching. Applying a potential difference between the electrodes in a molecular transport experiment gives rise to a considerable electric field. For a typical molecular length of 1 nm and a voltage bias of 0.5 V, we already get a field as high as 5×10^8 V m^{-1}. It has been shown that such a strong field can couple to a molecular dipole and the resulting force (torque) on the molecule can drive conformational changes, i.e. switching. For example, Zn(II) etioporphyrin can exist in two different (both non-planar) conformations on an NiAl(110) surface. Due to the alignment of the molecular dipole (perpendicular to the surface), an electric field can be used to switch the molecule in one direction [26].

2.2.4. Light-induced switching. When a molecule absorbs a photon, a transition to an excited state takes place. In the special case of a molecular switch, such an excitation can lead to an isomerization reaction (photoisomerization). In figure 2, we indicate how non-radiative relaxation can take place in the excited state, while the reaction coordinate changes accordingly. Finally, a transition to the ground state energy surface takes place. From there, the system relaxes further to one of the two minima. In a certain percentage of cases, this results in photoisomerization (if the 'other' minimum is reached). Clearly, this percentage depends on the fine details of the potential energy surfaces. For example, if an additional barrier exists in the excited state (unlike the smooth parabola in figure 2), switching rates may be strongly suppressed at low temperatures [30].

Photochromic switches form a clear example of molecules with an intrinsic switching mechanism. Generally, they are first tested in solution and then investigated in devices. Besides being attractive for future applications, e.g. light sensors, these molecular devices are of great interest from a fundamental point of view. The influence of the electrodes on the molecular switchability is only partially understood. In fact, several interaction mechanisms can play a role, from simple steric hindrance to energy transfer and charge transfer mechanisms. It is here that (mesoscopic) physics and (photo) chemistry meet.

2.2.5. Other stimuli. In some molecular systems, such as azobenzenes, the energy barrier between the two molecular states (see figure 2) is relatively low. In that case, it is, in principle, possible to switch a molecule by thermal excitation, i.e. heating. Such temperature-induced conversions are, in general, not very selective (switching will occur in both directions), unless there is a significant energy difference between the two isomers of the molecule (expressed in ΔG_{react} in figure 2). An interesting set of molecules that undergo a transition at a well-defined temperature are the so-called spin transition molecules [31–33]. Typically, these systems contain a transition metal ion and an organic ligand coordinated to it in an octahedral symmetry. As a result, the d orbitals of the metal split into the e_g and t_{2g} subsets, leading to two possible minimal energy states, with different spins. If the energy difference between the e_g and t_{2g} orbitals is greater than the electron–electron repulsion energy, the electrons occupy the lowest-energy orbitals (t_{2g}). Due to the Pauli principle, this leads to a low-spin configuration. In the opposite case, the d electrons occupy both the e_g and t_{2g} orbitals. Due to Hund's rules, this leads to a high-spin state. If the ligand field energy and electron–electron repulsion energy have similar values, it is possible to go from the low-spin to the high-spin state by heating. Moreover, the spin transition can also be influenced by pressure. In the high-spin state, the anti-bonding orbitals are partially occupied, which increases the bond lengths, leading to an effectively larger molecule. Hence, applying pressure favors the low-spin state, resulting in a higher transition temperature[5]. Performing well-defined charge transport measurements on spin transition molecules is a new challenge in the field of molecular transport. There are several groups working on these types of experiments, but there are still very few published results. Hence, we do not explicitly deal with spin transition molecules in the rest of this review. To get an idea of the (new) possibilities offered by transport experiments, we mention that some methods, such as the mechanically controllable break-junction technique may allow one to strain a molecule during the experiment. Furthermore, in three-terminal devices, a gate voltage may be used to control the ligand field energy, thus inducing a spin transition. First experiments in this direction have recently been performed [34].

2.2.6. Stimuli and directionality of switching. An important factor in the driving force for the switching is whether it can be used to control the direction of the switching reaction. Electrochemical potential control of the charging clearly will allow for this: different charge states have different conductivities and these can be selected by the electrochemical potential. It should also hold for electric-field-induced switching as the torque on the molecule depends on the direction of the electric field. In the case of light-induced switching, the situation is a little more complicated. Looking at

[5] For completeness, we note that light-induced switching from the low-spin to the high-spin state is also possible.

the typical potential energy curves for the ground and excited states of a two-level switch (figure 2), it is clear that the smaller energy (longer wavelength) photons can only induce switching in the downhill direction. Hence, sufficient illumination (how much exactly depends on the quantum yield) will result in full conversion. However, this is not generally true in the opposite direction. Finally, inelastic tunneling rarely allows for control, as it continually excites the molecule so that it can overcome the activation energy barrier in either direction. We note that the energy barrier is typically much higher than the energy of a single vibration, such that a 'ladder' of excited states needs to be climbed to overcome the barrier (vibrational heating). In some cases, it may be possible to control which vibrations (and where in the molecule) are excited, which can provide directionality.

2.3. Functionality and coupling

As introduced in figure 1, coupling a molecule to one or more electrodes can have a profound effect on its functionality, both in an positive and a negative way. Below, we elaborate on these two possibilities.

2.3.1. Functionality loss. Various phenomena can hamper the switching of a contacted molecule. First, there is a very fundamental issue. If a molecule is coupled strongly to electrodes, it is no longer correct to view the molecule as an isolated unit. One should rather consider the molecule and the first metal atoms as an 'extended molecule' with, in principle, a new set of 'molecular' energy levels (see below for more details). As a result, the pathway for molecular switching may change, in the extreme case becoming completely blocked. Let us take the example of a photochromic switch coupled to two electrodes. In such a device, the photo-excited electron and hole (exciton) may leak out to the electrodes on a timescale smaller than the time needed for a molecule to switch (typically $\sim$10 ps). Hence, molecular isomerization becomes very unlikely. Clearly, one way to prevent this is to decouple the molecular switch and the metal contacts electronically. This can be done by using a non-conjugated spacer. However, there is a price to pay for this: the 'on'-state conductance of the device will be reduced by several orders of magnitude when a large spacer is used. A second phenomenon to be taken into account is steric hindrance. Molecules that undergo a large conformational change upon switching may be mechanically hindered in their transition. A simple example is formed by molecules that undergo a large change in their effective length upon switching, such as azobenzenes. Fixed between two electrodes, such a molecule is likely to lose its functional properties. We note that steric hindrance can also be due to molecules neighboring the switch, e.g. in a self-assembled monolayer. These neighbors may be from the same or a different species (generally alkanethiols). Finally, a mechanism that plays a role in photochromic switches, such as azobenzenes and diarylethenes, is quenching due to electromagnetic dipolar coupling. The dipolar excitation in the molecular switch will see a mirror dipole in the electrodes. As a result, energy is transferred from the molecule to the metal, which may lead to failure of the light-induced switching process. This phenomenon is similar to the quenching of photoluminescence in the proximity of a metal and Förster resonant energy transfer [35]. Clearly, this type of quenching can be partially prevented by increasing the distance between molecule and electrode. However, the same considerations as described above apply: there is a trade-off between on-state conductance (strongly dependent on molecular length) and switchability.

2.3.2. Extrinsic switching. Remarkably, a molecular device may exhibit switchable properties even when a non-switchable molecule is contacted. The most trivial reason for this is that metal filaments are formed within the molecular layer. This phenomenon has been observed in several SAM-based devices, especially when evaporated top electrodes are applied [36–39]. Fundamentally more interesting are devices in which no filaments are formed, but switching is nevertheless observed. In this case, the device setting (or assembly on a surface) makes it possible to change the molecular conductivity by means that would not be possible in solution. For example, the switching may correspond to changes in the coupling between the molecule and one of the leads. We call such molecular devices extrinsic switches, to distinguish them from devices based on intrinsic molecular switches. The latter, e.g. photochromic switches, are chemically designed and tested for switchability in solution, before they are contacted by electrodes. Extrinsic switching is generally current-induced or field-induced. However, it is not always easy to distinguish the latter two, especially in a two-terminal geometry.

3. Charge transport through molecular junctions

In this section, we give a general introduction to the field of charge transport through molecular junctions. This lays the foundation needed to interpret the work on switchable molecular devices. This section consists of two parts. In the first, we discuss the basic theory of molecular charge transport. In the second, the main experimental methods are reviewed.

3.1. Basic models

When a molecule is connected to one or more electrodes, subtle changes in the molecular properties arise. As a result of metal–molecule coupling, the molecular orbitals can hybridize with the states of the metal contacts. Consequently, the original molecular levels broaden and shift compared to a free molecule in vacuum. This is illustrated in figure 4(a). An intuitive way to understand the broadening is via the Heisenberg uncertainty principle. Let us first consider a free molecule, where an electron occupies a level for a nearly infinitely long time τ. Hence, the uncertainty in its energy, ΔE, is almost zero. However, for a molecule coupled to an electrode, τ becomes finite as the lifetime of an electron on the molecule is limited by the molecule–lead coupling. Consequently, the uncertainty ΔE becomes significant, which translates into molecular level

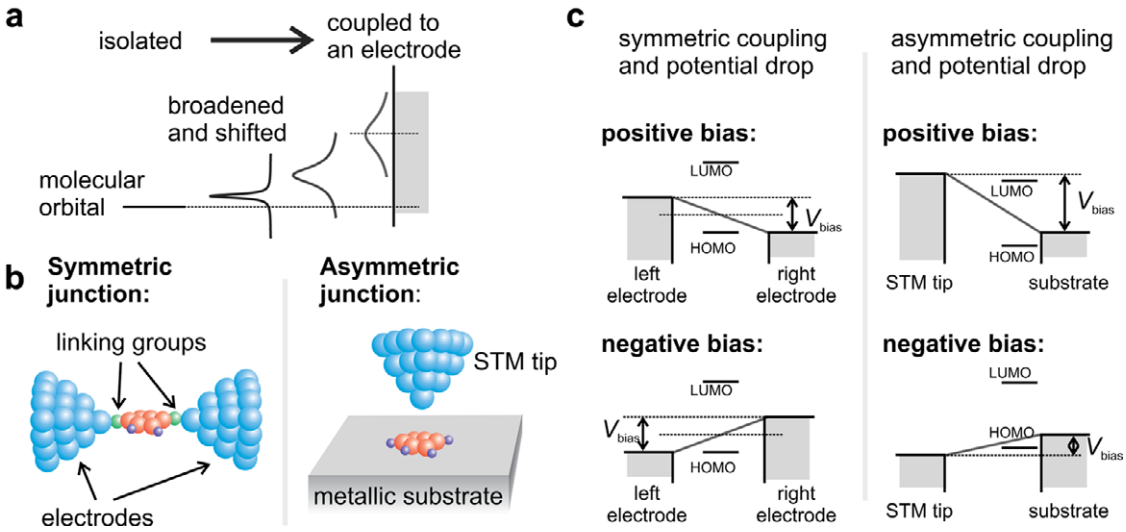

Figure 4. Theoretical background of molecular transport. (a) When a molecule is coupled to an electrode, its levels shift and broaden. (b) Schematics of a symmetric junction (left, typical for break-junction geometry) and asymmetric junction (right, typical for STM geometry). (c) The two limiting cases of coupling symmetry and potential distributions in metal–molecule–metal junctions: fully symmetric junction with $\eta = 0.5$ (left) and fully asymmetric junction with $\eta \approx 1$ (right).

broadening. For one level, the resulting molecular density of states $D(E)$ is given by a Lorentzian function [27, 40]:

$$D(E) = \frac{\Gamma/2\pi}{(E-\epsilon)^2 + (\Gamma/2)^2} \tag{1}$$

where ϵ is the energy of the modified molecular orbital. The total broadening is the sum of the coupling to each of the two electrodes Γ_1 and Γ_2, i.e. $\Gamma = \Gamma_1 + \Gamma_2$. We note that Γ_1, Γ_2 and thus Γ may be energy-dependent themselves. In the case of covalently linked molecules (chemisorption), the broadening can be several hundred meV, i.e. much larger than the thermal energy at room temperature (≈25 meV). Another effect of coupling a molecule to electrodes is partial charge transfer between the two. This causes the molecular levels to shift with respect to the free molecule and the shift can be different for orbitals with different symmetries. The problem of estimating the energetic position of the molecular orbitals relative to the Fermi energy of the electrodes is known as the level alignment problem, in analogy to the band line-up problem in semiconductor heterostructures [41, 42].

The interaction of the molecular orbitals with the electronic states of the electrodes is obviously of vital importance in determining the transport properties of the metal–molecule–metal junction. Typically, either the highest occupied molecular orbital (HOMO) or the lowest unoccupied molecular orbital (LUMO) dominate transport close to zero bias voltage. In general, transport is non-resonant, and the exact level positions determine whether it is the Lorentzian tail of the HOMO or the LUMO that carries most of the current. As the bias voltage is increased (or as a gate electrode is used to shift the molecular orbitals), resonant transmission through a molecular orbital may become possible. To determine the actual charge transport mechanism for a molecular junction, one has to consider the relevant energy scales. These are the thermal energy $k_B T$, the coupling energy between the molecule and the electrodes Γ and the charging energy U due to the Coulomb interactions between electrons on the molecule. In the limit of weak coupling, $U \gg \Gamma, k_B T$, electrons tunnel through the molecule one by one as their flow is controlled by electron–electron repulsion: addition of another electron is only possible if the energy barrier U is overcome [27, 40, 43]. In this regime, which is termed Coulomb blockade, the number of electrons on the molecule behaves as a classical variable with integer values and the transport can, in principle, be described by a master equation formalism. In the limit of strong coupling, $\Gamma \gg U$, transport is coherent and the number of electrons on the molecule is not well defined and subject to quantum fluctuations. To first order, the current through one (spin-degenerate) level can be calculated from the Landauer formula [27, 40, 43–48]:

$$I = \frac{2e}{h} \int T(E)[f(E-\mu_1) - f(E-\mu_2)]\,\mathrm{d}E \tag{2}$$

where $f(E)$ is the Fermi–Dirac function, $T(E)$ the transmission function given by $T(E) = 2\pi D(E)\Gamma_1\Gamma_2/\Gamma$ and μ_i the electrochemical potential of electrode $i = 1, 2$. At a bias voltage V_b, the chemical potentials are given by $\mu_1 = E_F + \eta e V_b$ and $\mu_2 = E_F - (1-\eta)eV_b$, so that $eV_b = \mu_1 - \mu_2$. The parameter η describes the symmetry of the voltage drop over the molecular junction. This is related to the strength and symmetry of the molecule–electrode coupling. As discussed below, there are two principal ways to contact individual molecules: in two-terminal junctions and by STM. These are illustrated in figure 4(b). From a theoretical point of view, they represent two different limiting cases: fully symmetric (ideal break junctions) and fully asymmetric junctions (STM). In the case of a symmetric junction, i.e. $\Gamma_1 \approx \Gamma_2$, about half of the applied bias drops on either side of the molecule and the chemical potentials of the leads shift by $\pm eV_b/2$ with respect to the molecular levels due to the

applied bias[6] ($\eta \approx 1/2$) [27, 49]. This leads to the situation illustrated in figure 4(c), left side: transport is dominated by one of the frontier molecular orbitals (HOMO or LUMO) at both positive and negative bias. In contrast, in an asymmetric junction (figure 4(c), right), Γ_1 and Γ_2 differ considerably and the molecular levels are 'pinned' to one of the electrodes (the substrate in STM). In that case, we have $\eta \approx 1$. In an experiment, the unoccupied levels are therefore probed at positive bias and the occupied levels at negative bias [50–53]. We stress here that, although there is a qualitative correlation between Γ_1/Γ and η, they are not the same. The Γ values represent electronic coupling, whereas η is related to the electrostatic potential profile, which can be obtained by solving the Poisson equation [54].

In many experiments, the derivative of the current with respect to the applied bias, $\mathrm{d}I/\mathrm{d}V_\mathrm{b}$, is measured directly by a lock-in technique. The lock-in technique boosts the signal-to-noise ratio compared to numerically differentiating the current and allows for extremely accurate data acquisition. Interestingly, the current derivative is directly proportional to the density of states. This means that it is possible to carry out electronic spectroscopy by measuring $\mathrm{d}I/\mathrm{d}V_\mathrm{b}$ versus V_b. Taking the derivative of the equation of the current (at 0 K), we find

$$\frac{\mathrm{d}I}{\mathrm{d}V_\mathrm{b}} = \frac{2e^2}{h}(\eta T(E_\mathrm{F} + \eta e V_\mathrm{b}) + (1-\eta)(T(E_\mathrm{F} - (1-\eta)eV_\mathrm{b}))). \tag{3}$$

This mathematically demonstrates the difference between symmetric and asymmetric coupling. If $\eta = 1$ (asymmetric coupling like in STM), the $\mathrm{d}I/\mathrm{d}V_\mathrm{b}$ versus V_b is proportional to the local transmission function at $E_\mathrm{F} + eV_\mathrm{b}$. If $\eta = 1/2$, however, a $\mathrm{d}I/\mathrm{d}V_\mathrm{b}(V_\mathrm{b})$ curve will be fully symmetric, regardless of the nature of the closest molecular orbital (HOMO or LUMO).

Besides the density of states, tunneling spectroscopy can also provide information on molecular vibrations. When the energy of the tunneling electron is sufficient to excite a molecular vibration, an electron–phonon interaction can cause some of the tunneling electrons to scatter inelastically. Interestingly, the effect that electron–phonon interaction has on the conductance depends on the value of the transmission function $T(E)$. Let us first consider tunneling contacts with small conductances, $T(E) \ll 1$. In that case, inelastic scattering results in an additional transport channel. Due to this extra transport channel, with conductance σ_inel, the differential conductance increases step-wise exactly at $eV_\mathrm{b} = \hbar\omega$: from $\mathrm{d}I/\mathrm{d}V_\mathrm{b} = \sigma_\mathrm{el}$ to $\mathrm{d}I/\mathrm{d}V_\mathrm{b} = \sigma_\mathrm{el} + \sigma_\mathrm{inel}$. Typically, this change is detected by recording the second derivative of the tunnel current $\mathrm{d}^2I/\mathrm{d}V^2$ as a function of V_b [22, 55–58]. Obviously, a step up in $\mathrm{d}I/\mathrm{d}V_\mathrm{b}$ results in a peak in $\mathrm{d}^2I/\mathrm{d}V_\mathrm{b}^2$ at positive bias. At negative bias, a dip is expected at exactly the same $|V_\mathrm{b}|$. This type of spectroscopy is called inelastic electron tunneling spectroscopy (IETS). Remarkably, when $T(E)$ is close to unity, inelastic scattering leads to the opposite effect, i.e. a decrease of the differential conductance. This effect, known originally from work on (quantum) point contacts, results from the fact that an ingoing electron that is inelastically scattered is necessarily reflected[7]. This type of spectroscopy, named point contact spectroscopy (PCS), has been pivotal in the characterization of junctions containing small molecules such as H_2 or even benzene [24, 59]. There has been some debate on the boundary between PCS and IETS. Recently, Tal *et al* showed that, for a single transport channel, a transition from step up to step down in $\mathrm{d}I/\mathrm{d}V_\mathrm{b}$ occurs when the transmission function has a value $T(E) = 1/2$ [60]. Nevertheless, both in IETS and PCS, coupling to different vibrational modes depends both on the symmetry of the mode and the symmetry of the underlying electronic orbital [61–63]. Electron–vibration coupling can also be observed in resonant transmission. The coupled electron–vibration states are called vibronic states and they result in the appearance of a phonon replica in the $\mathrm{d}I/\mathrm{d}V_\mathrm{b}$ spectra [20, 64–66], in analogy to electron–phonon coupling in transport through quantum dots [67, 68]. Finally, we repeat that continuous excitation of molecular vibrations may lead to a change of the molecular configuration in the device. Hence, this form of switching is closely related to IETS, PCS and vibronic excitation. As a closing remark of this section, we refer the interested reader to various more in-depth reviews on molecular transport and its theory [27, 43, 45–47, 69, 70].

3.2. Experimental techniques

There are two main approaches to study charge transport through molecules experimentally. First, one can apply scanning tunneling microscopy (STM) to investigate molecules on a surface. Second, one can probe molecules in two-terminal metal–molecule–metal devices[8]. In an STM experiment, the molecules are deposited on a surface, which defines the first contact. The STM tip provides a weaker tunnel contact to the molecule (no chemical bond). In the two-terminal approach, one creates a more symmetric device with direct coupling—through chemical bonds—between the molecule and both electrodes. A gate electrode may be added to control the molecular level position with respect to the Fermi levels of the electrodes. Over the past years, the combination of STM-based studies and molecular device research has proven essential for the progress of molecular electronics in general and for the research on switchable molecules in particular. We will emphasize the strengths of each technique and point out how they can be used to obtain complementary information on the operation of molecular switches. Our treatment of the various methods to study charge transport through molecules will be relatively brief. For a more extended discussion, we refer to the excellent reviews by Chen *et al* [47], Akkerman and de Boer [71], Kröger *et al* [72] and Prokopuk and Son [73].

[6] We note that, even in two-terminal junctions, coupling is generally not fully symmetric.

[7] Basically, the reason for this reflection is that all ingoing states are occupied for energies lower than the original electron energy. Only the distribution function of reflected electrons (opposite momentum) has empty states at the lower electron energy. Hence, the scattered electron has no choice but to occupy one of the latter states at opposite momentum and thus get reflected.

[8] If a gate is present in such a device, one generally speaks of a three-terminal device, the gate being the third electrical connection.

3.2.1. Scanning tunneling microscopy. Since its conception in the early 1980s, there have been few techniques in the physical sciences that have had as large a conceptual impact as scanning tunneling microscopy [74, 75]. In the beginning of its development, the impact of STM was in providing atomically resolved images of well-defined surfaces, such as single crystals. However, the past decade has seen an enormous increase of STM studies focusing specifically on the properties of single molecules and nanostructures [76–80]. It is fair to say that STM has established itself as the premier research tool in nanoscience. The strength of STM lies in the combination of high-resolution imaging (STM) and spatially resolved electrical spectroscopy (scanning tunneling spectroscopy, STS), which is capable of providing the local density of states (LDOS) with atomic spatial resolution [78, 81, 82].

In figure 5(a), we schematically present the STM technique. In the STM mode, the tip scans the sample surface while recording the tunnel current at a chosen bias V_{bias}. This voltage refers to the potential of the substrate with respect to the tip. Scanning can be done in either the constant-height or the constant-current mode. In the constant-height mode, the tip stays at the same height during scanning, while changes in the tunnel current are recorded. In the constant-current mode, the tip height is controlled by a feedback loop such that the tunnel current between tip and substrate is maintained constant. It is important to realize that the resulting 'apparent height' image contains information on both the electronic and topological properties ('true height') of the sample. This can be easily understood. On the one hand, the coupling matrix element between the STM tip and the surface depends exponentially on their separation: $\Gamma_1 \propto \exp(-2\kappa d)$, where κ is the decay constant. For a vacuum barrier, the tunnel current decreases by roughly one order of magnitude per Å. On the other hand, the tunnel current depends on the local density of states $D(E)$ [83–87]. Hence, a conjugated molecule may appear higher than a non-conjugated molecule of the same size. In fact, resonant transmission through a molecular orbital can lead to an increase of the apparent height by several ångströms.

STM studies are performed in a broad range of conditions, dependent on the specific scientific questions asked: in ultra-high vacuum (UHV) at low temperatures or at room temperature, in liquid or in ambient conditions. Figure 5 shows two types of STM experiments on single molecules. They differ in the way the molecules have been assembled on the surface. For most of the STM experiments performed at low temperature and/or under UHV conditions, molecules are deposited onto a substrate *in situ*. This usually results in molecules lying flat on the surface (see figure 5(a)). Spectroscopy can be performed by recording the current I or the differential conductance $\mathrm{d}I/\mathrm{d}V_{\mathrm{b}}$ at a given position over the molecule, while V_{b} is varied. In addition, as was pointed out in the previous section, transport experiments can be used to obtain information on the molecular vibrations. In the STM set-up, it is even possible to spatially resolve where current injection leads to vibrational excitation [55, 56, 65]. Remarkably, such electron–phonon interaction also opens up the possibility to manipulate single molecules. In some specific

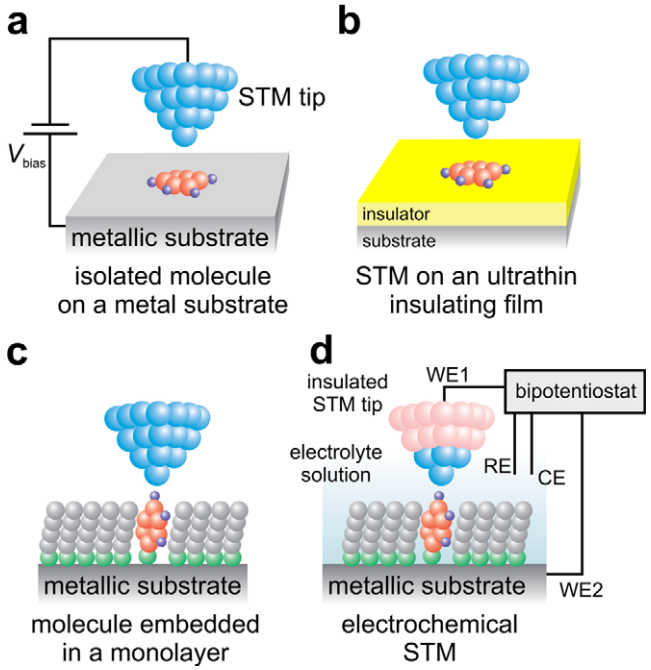

Figure 5. Schematic of STM experiments on single molecules. (a) STM experiment on a molecule lying flat on a substrate (typically a metal single crystal). (b) STM on a molecule deposited on an ultrathin insulating film. In stable conditions (low temperature, ultra-high vacuum), molecular orbitals can be resolved and spectroscopically studied. (c) STM experiment on a diluted self-assembled monolayer (SAM). A conjugated molecule is isolated within a matrix of alkanethiols. Upon scanning such a sample in constant-current mode, the conjugated molecule is distinguished by its different apparent height h_{app}. Since h_{app} is a convolution of true physical height and conductance properties, changes in h_{app} can qualitatively be related to molecular switching. (d) Electrochemical STM. STM is carried out in an electrochemical cell where a bipotentiostat can be used to the control the potential of both the tip and the substrate with respect to a reference electrode in solution (electrochemical gating).

cases, it has been shown that one can break atomic bonds and move atoms within a single molecule [12, 88].

One can reduce the coupling between the metal substrate and the molecule by introducing an ultrathin insulating layer on the substrate (see figure 5(b)). Popular choices for the insulating material include Al_2O_3 [14, 52, 65, 89], NaCl [12, 13, 78, 90] and Cu_2N [91, 92]. The reduced coupling makes it possible to image molecular orbitals and study them spectroscopically with impressive spatial and energy resolution [12, 78, 90, 93].

An alternative approach in STM is to probe one end of a molecule that is standing (nearly) upright on a substrate. This makes it possible to study charge transport in the length direction of the molecule, i.e. somewhat similar to a two-terminal device (see figure 5(c)). Such a geometry can be achieved by using self-assembled monolayers (SAMs) of the molecules of interest. If molecules are functionalized by linker groups that can bind to a metal surface, they spontaneously form such monolayers from solution. The stereotypical example is the formation of SAMs of thiol-derivatized molecules on gold [94–96]. The structure and

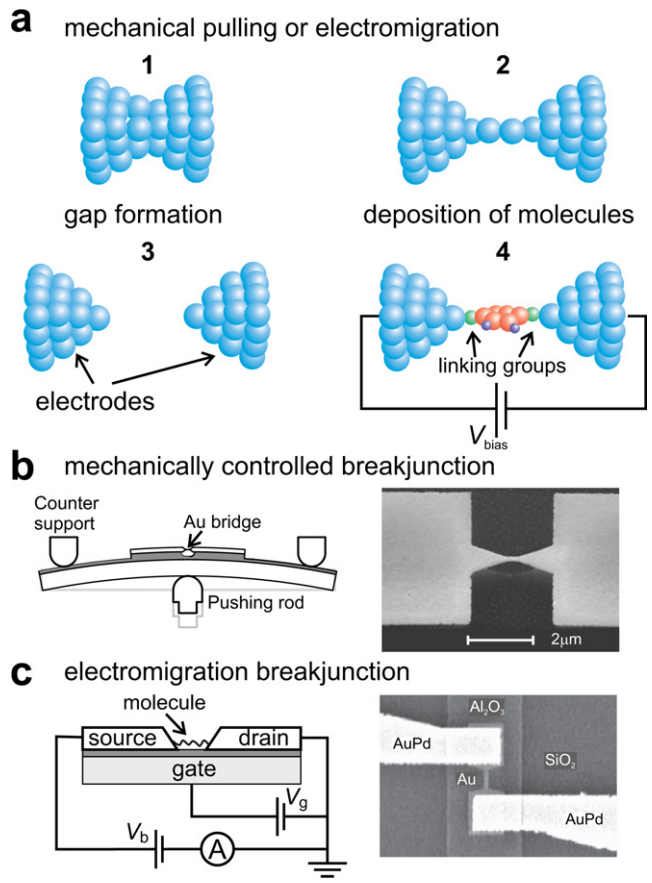

Figure 6. Break-junction techniques for studying charge transport through single molecules. (a) Formation of a nanometer-scale gap followed by insertion of the molecules of interest. The gap may be created by mechanically breaking the constriction (see (b)) or by electromigration (see (c)). (b) Mechanically controllable break junctions. Left: three-point bending configuration. Right: scanning electron microscopy (SEM) image of a lithographic mechanically controllable break junction. Upon bending the substrate, the constriction is first elongated and finally broken. This produces two clean electrodes, the distance between which can be accurately controlled by the pushing rod. (c) Schematic (left) and an SEM image (right) of an electromigration break junction with a gate electrode separated from the molecule by a thin insulating layer. In this case, a gap is enforced by electromigration, i.e. atomic diffusion biased by an electric field. Adapted with permission from [19]. Copyright 2007, American Chemical Society.

order of such SAMs depends on the length, cross-sectional area and flexibility of the molecules. For example, straight chain alkanethiols form fully ordered, crystalline monolayers on gold. The drawback of this method is that the molecules in the close-packed monolayer can interact and their properties can differ from those of individual, isolated, molecules. This can be overcome by mixing the molecules of interest into an inert matrix of molecules with a large HOMO–LUMO gap, typically alkanethiols. As first demonstrated by Bumm *et al*, an island of isolated conjugated molecules (ideally a single molecule) can be inserted within the SAM by performing a subsequent self-assembly step (see figure 5(c)) [97]. If both types of molecules are chosen to have the same physical length, the conjugated molecule can be distinguished in STM by its larger apparent height h_{app}. As explained above, this is due to the fact that h_{app} is a convolution of topology and electronic properties of the molecule under the STM tip. Hence, this type of STM experiments allows one to get information on the relative conductance properties of the isolated molecules, for example as a function of their length or binding group [98]. This makes the method quite attractive to study molecular switching. Indeed, as a molecule is converted from a high conductance to a low conductance state, h_{app} changes significantly in a step-like fashion from high to low and vice versa [99–106]. However, it must be borne in mind that interpretation of the data should be done carefully, especially for conformational switches. The main reason for this is that it is not possible to independently measure the change in the physical height of the isolated molecule (or in its angle with respect to the surface). This makes it difficult to obtain the conductance change upon switching quantitatively. Nevertheless, STM on diluted SAMs is a good method to study single molecules qualitatively under realistic conditions (in air or in a liquid). In contrast to the two-terminal device experiments discussed below, however, there is always a tunnel gap between the molecule and the STM tip, i.e. the molecule is covalently bound to only one electrode.

While it is challenging to integrate a gate electrode in the STM set-up in air or vacuum, it is possible in liquid using an electrochemical STM (figure 5(d)). This experimental set-up (typically at room temperature) involves carrying out STM in an electrochemical cell, in an electrolytic solution. The potential of the STM tip and the substrate is controlled with respect to a reference electrode by a bipotentiostat. The thickness of the electrochemical double layer is given by the Debye length in solution, which depends on the electrolyte concentration. For sufficiently high electrolyte concentrations, this length is small (∼1 nm) and the molecule can be charged in the STM tip–substrate gap. This makes it possible to use the potentiostat to control the charge of the molecule, in analogy to an electrostatic gate electrode in three-terminal transport experiments.

3.2.2. Metal–molecule–metal devices. Contacting a nanometer-scale molecule symmetrically by two electrodes is not a trivial task. Nevertheless, many ingenious techniques have been devised by a broad range of groups (see figure 6). Below, we briefly discuss the most viable methods.

Controllable break junctions. Controllable break junctions are devices in which the distance between two electrodes can be controlled with impressive accuracy [23]. This tunability makes them perfectly suitable to 'catch' single molecules of a given length (see figure 6(a)). We first discuss mechanically controllable break junctions (MCBJs), which have been pioneered by Moreland and Ekin, and Muller and Van Ruitenbeek [107, 108]. Basically, an MCBJ consists of a metal wire (e.g. gold) with a narrow constriction, fixed on top of a flexible substrate. This substrate is put in a three-point bending geometry, where it can be bent by moving a pushing rod upwards (see figure 6(b)). As the substrate is bent, the metallic wire is elongated until finally the metallic constriction breaks and two fresh electrode surfaces are created. Conveniently, the distance between these two

electrodes is linearly related to the pushing rod position, via a reduction factor r. For so-called 'notched' or 'classical' MCBJs, a carefully prepared metal wire (diameter $\sim$50 μm) is used. In this case, r is relatively large ($0.001 < r < 0.1$). To obtain a good control of the inter-electrode distance, the pushing rod is therefore translated by a piezo-element. For 'nanostructured' or 'lithographic' MCBJs, the constriction in the metal wire is defined by electron beam lithography. As a result, the reduction factor r is very small ($10^{-6} < r < 10^{-4}$), leading to improved distance control and impressive mechanical stability [109–112]. Besides MCBJs, a hybrid type of controllable break-junctions can also be defined: STM-controlled break junctions (STM-BJs). Here, it is an STM tip that is used to chemically connect to molecules or atoms on a conducting substrate. The distance control between the two electrodes (substrate and tip) is provided by the piezo-scanner of the STM. Compared to MCBJs, STM-BJs have a reduction factor of unity, which makes them mechanically somewhat less stable (in the open-loop mode). On the other hand, STM-BJs do offer the advantage of performing STM scans before junction formation, to inspect the local environment.

Many of the pioneering studies on single atomic junctions have been performed using controllable break junctions [23, 107, 108, 112–114]. The impressive results obtained inspired Reed and Muller *et al* to use nanostructured MCBJs to study charge transport through single benzenedithiol molecules [115]. Their work has led to a series of fascinating experiments on a variety of organic molecules, which all make use of the gold–thiol chemistry to connect molecules and electrodes [49, 110, 115–125]. In parallel, the Van Ruitenbeek group adapted the classical MCBJ method to study small inorganic molecules, such as H_2, D_2, and H_2O, applied from a gas/vapor [24, 59, 60, 126, 127].

Operating molecular devices in solution opens the possibility of *in situ* chemical reactions or electrochemical control of redox switching. This is one of the main reasons why Xu and Tao extended the break-junction method to organic molecules in solution [128]. By moving a gold STM tip in and out of contact with a gold substrate in a solution of dithiol molecules, molecular junctions could repeatedly be formed (STM-BJs). Histograms of the conductance evolution during breaking provided evidence for the formation of molecular junctions. Recently, further studies to explore molecular junctions in solution have been carried out [47, 110, 120–125, 129–139]. An important contribution was made by Venkataraman *et al* who provided evidence for improved molecular junction formation when amine coupling groups are used with gold electrodes [138, 139]. Indeed, the search for the ideal coupling groups is an on-going quest in this field. Finally, we mention two methods, which are gentler varieties of the STM-BJ technique. First, Haiss *et al* employed a liquid-cell STM set-up to investigate a submonolayer of dithiol molecules on a flat gold surface [140, 141]. Very roughly speaking, they use an STM tip to 'fish' for a dithiol molecule lying flat on the surface, either actively (by moving the tip in and out of contact) or passively (by waiting for a molecule to connect and disconnect spontaneously, see also [142]). Inspired by the same philosophy, the Tautz group demonstrated molecular junction formation at low temperatures, by lifting up flat-lying molecules at one side, with the STM tip [143]. A similar experiment was performed by Lafferentz *et al* who studied single polyfluorine molecules. The latter had formed from the monomers by a polymerization reaction on the Au(111) surface [144].

Other single-molecule devices. Several other methods to create molecular junctions have recently been designed. A very influential method is due to Park *et al* [145]. It is based on electromigration, i.e. biased diffusion of atoms, vacancies or interstitials in the presence of an electric field [146–148]. Electromigration can be used to break a gold wire, covered with the molecules of interest (see figures 6(a) and (c)). If performed properly, distances of around 1 nm can be realized between the two freshly created electrodes, so that a molecular bridge can subsequently connect the electrodes. Because of its apparent simplicity, this method has been generally applied to measure molecular transport properties [19, 20, 149–151]. Nevertheless, the technique should be used with care. During electromigration the junction heats up locally, even in liquid helium [152–154]. This may lead to both the destruction of molecules and the formation of gold nanoparticles [153, 155, 156]. By using an appropriate feedback scheme, uncontrolled breaking of the wires can be prevented [148, 154, 157–159].

In 1999, Morpurgo *et al* proposed electrodeposition as a method to create two electrodes with nanometer distance [160]. The inter-electrode distance can be tuned on the atomic scale in an aqueous solution by depositing (or removing) atoms at a low rate. Kervennic *et al* created molecular junctions with this technique [161]. Another method to control the inter-electrode distance on the atomic scale has been designed by Kubatkin *et al* [162]. Using a shadow mask and evaporation at variable angles in UHV, they obtained well-defined molecular devices under very clean conditions and at low temperatures.

Devices using nano-objects as intermediates. A number of groups have based their designs on a somewhat different philosophy. Pointing to the inherent size difference between electrodes (width $\sim$200 nm) and small organic molecules ($\sim$nm), they propose to bridge this gap by intermediate-size objects. Many successful methods have been designed, e.g. using carbon nanotubes [163, 164], microparticles [165] or nanoparticles [166–177]. Specifically, the Nuckolls group demonstrated how individual molecules can be trapped within a single-wall carbon nanotube that has been locally cut by oxidative etching (see figures 7(a) and (b)). The nanotube itself is connected to two larger metallic electrodes (originally Au) [163, 164]. Another important contribution was made by Dadosh *et al*, who managed to contact and characterize particle–molecule–particle dumbbells from solution [167]. Several groups have recently focused on two-dimensional networks of nanoparticles, building on the pioneering work by Andres *et al* [166, 169–175, 177, 178]. It was shown that dithiolated organic molecules can form bridges between neighboring nanoparticles, which themselves can be assembled to form highly ordered triangular lattices (see figures 7(c) and (d)) [166, 171–173, 177]. These larger molecule–nanoparticle sheets are contacted by evaporated

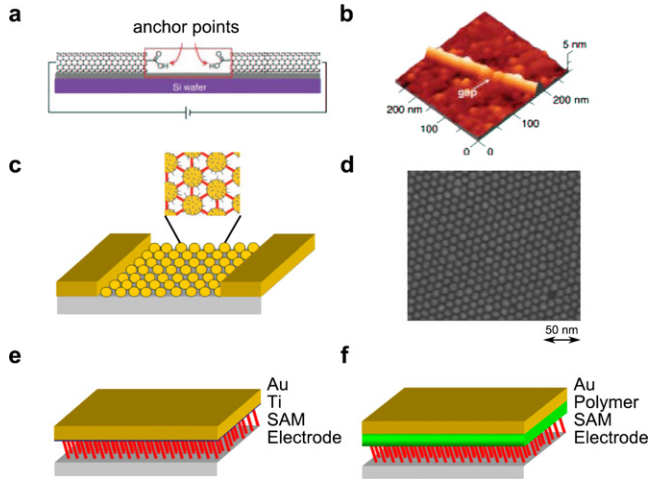

Figure 7. Molecular device structures. (a) Schematic picture of an etched carbon nanotube. The resulting gap can be bridged by one or a few molecules connecting at the carboxyl groups. The nanotube itself is contacted by metal electrodes in turn. (b) Atomic force microscopy (AFM) image of an etched nanotube. The gap is just visible. From [163]. Reprinted with permission from The American Association for the Advancement of Science. (c) Regular two-dimensional electrodes. Nearest-neighbor particles are connected by molecular bridges (see inset). In this way, the system forms a 2D assembly of single metal–molecule–metal junctions [166, 171]. (d) Scanning electron micrograph of an actual nanoparticle network (scale bar: 50 nm). (e), (f) Self-assembled monolayer (SAM) devices. The device consists of a bottom electrode, usually gold, on top of which a SAM has grown. Creating a well-defined top electrode is the most challenging part. Initially, Ti/Au stacks were often used (e), but their stability was strongly questioned. To solve this issue, other top electrodes have been proposed, including a conducting polymer layer (f) [190, 192].

electrodes in turn. Apart from their impressive stability, these networks offer the possibility of optical control experiments (infrared, Raman or UV–vis) to confirm the presence of the molecules [172, 174, 177].

Devices based on self-assembled monolayers. Several groups have concentrated on studying self-assembled monolayers (SAMs) of thiolated molecules in a two-electrode geometry. Here, the idea is to create an SAM on a gold layer (the first electrode), which is subsequently contacted by a top electrode. In such a device, many molecules (typically from a few thousand upwards) are probed in parallel. Initially, most studies used a top contact which had been evaporated directly on top of an SAM (see figure 7(e)). However, it turned out that this method should be used with great care, since otherwise metal filaments grow and/or chemical reactions (metal carbide formation) take place [36–39]. Various creative methods have been introduced to circumvent this problem. First, nanocontact printing has been used as a soft-lithographic approach to create a stable top contact on an SAM [179, 180]. Alternatively, Rampi and Whitesides have made use of Hg droplets, covered by a second SAM, as a top electrode [181–184]. This method has the great advantage that it is flexible and simple. However, the presence of a second SAM does have to be taken into account in the analysis. A third approach has been explored very successfully by Kushmerick and co-workers [185, 186]. Their 'crossed-wire' method makes use of two thin wires at a 90° angle. One of the wires is covered by the SAM of interest. An external magnetic field is applied perpendicular to the direction of this wire. Upon applying a current through this wire, the resulting Lorentz force gently presses the wires into physical contact, creating a metal–SAM–metal device. The stability of these devices allowed for detailed study of several SAMs by inelastic tunneling spectroscopy [58]. Finally, we refer to the technologically very impressive work on nanoscale cross-bar devices by Heath and co-workers (see the section on mechanically interlocked switches for more details) [187–189].

Very recently, it has been demonstrated that stable SAM-based devices can be created by using a conducting polymer layer as a top electrode. In this way, filament formation as well as spurious chemical reactions between top electrode and SAM are completely prevented (see figure 7(f)). Akkerman *et al* used PEDOT:PSS (poly[3,4-ethylenedioxythiophene] stabilized with poly[4-styrenesulfonic acid]) as a top polymer electrode to create large area structures with great potential as functional devices [190, 191]. Furthermore, Milani *et al* used PmPV (poly[(*m*-phenylenevinylene)-*co*-(dioctoxy-*p*-phenylenevinylene)]) as a top electrode. The PmPV is in turn contacted by an Hg droplet. Hence, the second SAM needed for the original Hg-droplet method is no longer necessary [192].

4. Transport studies on switchable molecules

In this section, we review transport studies on switchable molecules. Interestingly, many of the early reports on molecular conductance switching relied on an extrinsic mechanism. In addition, in some cases it has later been realized that the mechanism is extrinsic rather than intrinsic. For this reason, we will first discuss examples of extrinsic switching. Then, we will change our focus to switching based on an intrinsic molecular mechanism.

4.1. Extrinsic switches

The first type of a well-defined switch on the nanoscale consisted of a single Xe atom on Ni(110) studied at low temperature in an ultra-high vacuum STM [25]. This is clearly an example of extrinsic switching: the switch is based on controlled transfer of Xe atoms between the nickel surface and tungsten STM tip. These two configurations give rise to different conductivities and the position of the atom can be switched in a controlled fashion by applying higher positive or negative bias. The current and voltage dependence of the switching rate was found to be consistent with vibrational heating.

In another early example of extrinsic molecular switching, researchers used the manipulation capability of STM [193, 194] to study how the conductance of a molecule depends on its conformation. Moresco *et al* described the use of a specifically designed porphyrin-based molecule functionalized with four bulky di-(ter-butyl)-phenyl-groups [195]. Normally, these groups adsorb in a flat configuration with both the ter-butyl-groups in contact with the substrate. However, the di-(ter-butyl)-phenyl legs of the porphyrin can be rotated by either

moving the tip over the molecules at low tunneling resistance, or by pushing one of the legs with the tip. This rotation of the leg results in a decrease of over an order of magnitude in the tunneling resistance.

Another important example of extrinsic molecular switching is the behavior of oligo(phenylene ethynylene) (OPE) molecules. These molecules were found to exhibit stochastic switching in room temperature STM experiments on diluted SAMs [99] (see figure 8). The authors used a dodecanethiolate monolayer matrix as a host to contain, support and isolate derivatized OPE molecules. They compared related molecules (different side groups) that had demonstrated switching behavior in nanopore experiments (nitro-, and nitro- and amino-substituted), with those that had not (unsubstituted 4-4′-di(ethynylphenyl)-1-benzenethiolate) [99, 196]. Surprisingly, the authors found that all the molecules exhibited random or 'stochastic' switching behavior. They also correlated the switching rate with the amount of conformational freedom the molecules have. Molecules with higher degrees of conformational freedom exhibited higher switching rates. While the conclusion was that the switching is not related to the substituents, one of the molecules (4-4′-di(ethynylphenyl)-2′-nitro-1-benzenethiolate) allowed limited control of the switching by the electric field. A possible explanation for these results was given by the observation of stochastic switching in simple alkanedithiols embedded in alkanethiolate SAMs [101]. Such switching in alkanethiols cannot be caused by internal molecular electronic changes and consequently, these authors argued that the switching is caused by changes in the thiol bond between the molecules and the gold substrate. They dubbed the result 'the blinking of a thiol–gold bond'. Stimulated by this suggestion, the groups of Weiss and Tour investigated the stochastic switching of OPE molecules in more detail [100, 197–199]. Through careful engineering of the molecular dipole, and the interactions between the molecular switch and the matrix molecules, the authors were in fact able to tailor the behavior of the switch [100, 197]. It was shown that the direction of the dipole moment controlled the bias polarity dependence of the switching, i.e. whether 'on' or 'off' state was preferred at positive or negative bias. In addition, hydrogen bonding interactions between the OPE and matrix molecules were found to be necessary for observing bias-dependent switching. By expanding the set of studied molecules, they identified a change in hybridization of the molecule that occurs with a change in the molecule–substrate contact as the only explanation consistent with all experimental observations [198]. For completeness, we note that several other groups have connected stochastic switching to conformational and orientational changes of the inserted molecules, possibly due to the high local electric field [102, 104]. The Zandvliet group, however, relate the blinking effect of phenylene ethynylene molecules to lateral diffusion and exchange of conjugated molecules [200][9].

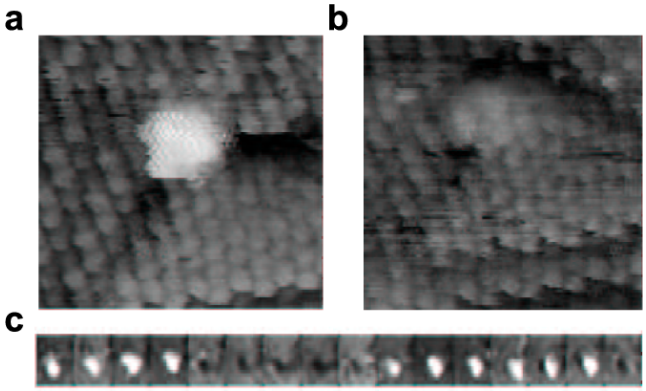

Figure 8. Stochastic (random) switching as observed by ambient STM. (a) OPE–thiol molecule in the 'on' state (bright protrusion) in a matrix of dodecanethiols (small dots). (b) The same OPE molecule in the 'off' state (note the decrease in apparent height). (c) Stochastic switching between 'on' and 'off' states (different molecule than in (a) and (b); time interval: 6 min per frame). From [99]. Reprinted with permission from The American Association for the Advancement of Science.

An interesting contribution related to the work on OPEs is by Blum *et al* [201] They used three independent techniques (STM, crossed-wire and magnetic-bead junctions) to demonstrate that molecules similar to OPE, namely bipyridyl-dinitro oligophenylene–ethynylene dithiol (BPDN, see figure 9(a)), show two distinct types of switching behavior: stochastic switching in analogy to OPE (which was also investigated in this study) and voltage-triggered switching, which was not observed with OPE. In break-junction experiments at low temperature, Lörtscher *et al* showed that stochastic switching of BPDN is suppressed and they were able to controllably and reversibly switch BPDN molecules between two conductance states [118] (see figure 9(b)). In addition, they demonstrated that controlled switching behavior can be used to write, read and erase bits by simple voltage pulses and hence to employ a single BPDN molecule as a memory element (see figures 9(c) and (d)). As a background check, a related molecule without the nitro groups, bipyridyl oligophenylene–ethynylene dithiol, did not show any switching behavior. Despite this indication on the importance of the nitro groups for the molecular switching, it is not clear what the exact mechanism in the case of BPDN is. Electrostatic charging, conformational changes or voltage-induced breaking of the bonds of the tethered molecules at the surface have all been proposed [15, 118, 201]. It is clear that the local chemical and structural environment of molecular electronic components is crucial for optimizing their function. Moreover, the role of the contacts can be vital in determining the function of a molecular-scale device. A very different example of the latter was reported by Quek *et al* [202]. They made use of the STM–break-junction geometry to create a

[9] Interestingly, a very different example of stochastic switching was recently demonstrated by Osorio *et al* [271]. They studied grid-like [2 × 2]-Co_4^{II} molecules in three-terminal devices and observed random switching events between stable branches, provided a certain threshold voltage was applied. The authors connected this type of stochastic switching to subnanometer movement of the BF_4^- counterions used to stabilize the molecule of interest. From a more general point of view, this work emphasizes that the behavior of counterions should always be taken into consideration to interpret molecular transport studies.

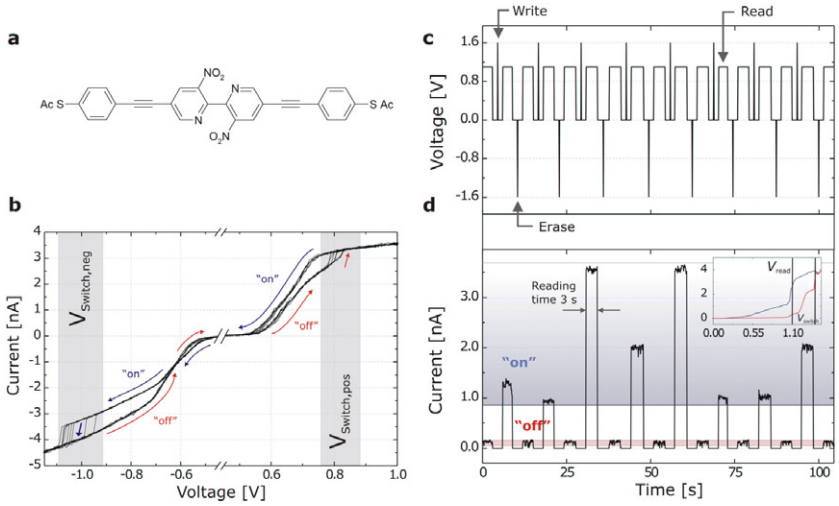

Figure 9. Controlled switching of a BPDN–dithiol molecule (shown in (a)) contacted in an Au break junction (MCBJ), at 100 K. (b) Hysteretic $I(V)$ (current–voltage) curves. If the voltage applied exceeds a positive threshold value ($V_{\mathrm{Switch,pos}}$), switching from the initial 'off' to the 'on' state occurs. A negative voltage sweep or a pulse below the negative threshold value ($V_{\mathrm{Switch,neg}}$) resets the molecule to the initial 'off' state. (c), (d) Memory operation based on the hysteretic $I(V)$ curves. (c) Write, read and erase voltage pulse pattern applied. (d) Resulting switching between 'off' and 'on' state. This molecular junction is different than the one in (b). The inset shows its $I(V)$ curve. From [118]. Reprinted with permission from Wiley. See also the work by Blum *et al* [201].

gold-4,4-bipyridinegold molecular device (note: N–Au bond). Quek *et al* demonstrated reversible toggling between two conductance values upon junction elongation and compression. Using first-principles calculations, the two conductance states were related to two distinct contact geometries at the nitrogen–gold bond.

To end this section, we discuss a case of extrinsic switching in an extremely simple molecule with practically no internal degrees of freedom. Recently, Trouwborst *et al* demonstrated controlled conductance switching in Au–H_2–Au break junctions at low temperature (see figure 10) [203]. This research built on earlier work by Thijssen and Halbritter *et al*, who had reported fast two-level conductance fluctuations in Au–H_2–Au junctions, when a bias of 40 mV or more is applied [126, 204]. (Interestingly, similar features have also been observed and analyzed in Ag-C_{60}–Ag junctions, though at different biases [205]) The bandwidth of the electronics being limited, this generally led to the observation of a step up (or a step down) in the molecular $I(V)$ curves (see figure 10(a), top curve). Thijssen *et al* used hydrogen isotopes to demonstrate that this step is related to the excitation of a molecular vibration. The different conductance states are most likely due to different configurations of the H_2 molecule with respect to the two electrodes. Trouwborst *et al* showed that by stretching such an Au–H_2–Au junction, a stable hysteresis loop in the $I(V)$ curves arises (see figure 10(a)). Using this hysteresis as a basis, a highly controllable and extremely stable conductance switch could be demonstrated (see figures 10(b)–(d)). The authors propose that the hysteresis results from a difference in the hydrogen phonon energy for the two configurations involved, the vibrational energy being lower for the second, metastable configuration [203].

Summarizing, extrinsic switching is a surprising phenomenon that opens up new possibilities of creating a functional molecular device. Scientifically, many of the effects

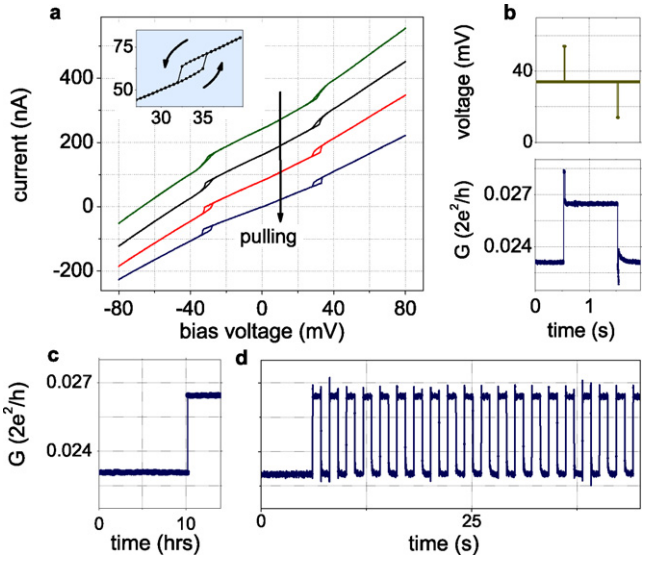

Figure 10. Controlled switching in an Au–H_2–Au junction at 5 K. (a) When the junction is pulled on by ≈2 Å, a time-independent hysteresis develops from a step up in the $I(V)$ curves. For clarity, the subsequent curves are shifted vertically. Inset: detail of a hysteretic curve. (b) Hydrogen switching based on the hysteretic $I(V)$ curves. Upper graph: voltage used to control the switch. On top of an offset voltage (34 mV), the voltage is pulsed by +20 mV (to go from 'off' to 'on') or −20 mV (vice versa). Lower graph: response. (c) Stability of the hydrogen switch. No decay occurs on the timescale of hours. After 10 h, switching from 'off' to 'on' is performed. (d) Multiple switching cycles. Up to 5000 cycles have been demonstrated. The duration of all pulses used in (b)–(d) is 20 ms. Reprinted with permission from [203]. Copyright 2009 by the American Physical Society.

seen are only poorly understood. In some cases, this is due to experimental limitations, making it hard to distinguish different switching mechanisms convincingly. Nevertheless, in

most cases, there is fascinating science waiting to be explored in detail, both experimentally and theoretically.

4.2. Tautomerization

As explained in section 2.1, conformational switches are based on bistability of the molecular geometry. This can be achieved through either stereoisomerization or structural isomerization of the molecule. An elegant example of structural isomerization is given by molecular switching in naphthalocyanine, which is induced by a hydrogen tautomerization reaction. This refers to migration of hydrogen atoms within the molecule, resulting in two different configurations (tautomers) with different conductances. Figure 11(a) shows I and $\mathrm{d}I/\mathrm{d}V$ versus bias voltage V_b measured on a naphthalocyanine molecule (see figure 3(c)), adsorbed on an ultrathin insulating film on a copper single crystal [12]. The insulating film (two monolayers of NaCl) serves to isolate the molecule from the metallic substrate, which results in clear resonances corresponding to tunneling through the HOMO and LUMO of naphthalocyanine in the measured spectrum. The molecular orbitals could also be imaged in real space (figure 11(b)), and comparison with DFT calculations on isolated molecules demonstrated that the electronic structure of an essentially isolated molecule could be probed [12, 78]. When the V_b was increased significantly above the LUMO orbital, the current unexpectedly oscillated between two stable values (figure 11(c)). By reducing the bias voltage back to the LUMO resonance and directly imaging that orbital, the authors could show that the switching reaction corresponds to the hydrogen tautomerization reaction of the inner hydrogens of the naphthalocyanine molecule (figure 3(c)). The reaction formally corresponds to a rotation of the hole molecule by 90°, but it is only the hydrogens that move without changes in the outer framework of the molecule. The hydrogen atoms break the fourfold symmetry of the molecule and the tautomerization reaction causes all the electronic orbitals to rotate by 90°. When the bias is set such that tunneling proceeds through one (or a few) orbitals, the tautomerization reaction results in considerable changes in the conductance.

It was shown that the tautomerization of the inner hydrogens is induced by the tunneling current, i.e. by an inelastic single-electron process. The linear dependence of the switching rate on the current (at a fixed bias) is consistent with a single-electron process. By measuring the switching rate at different positions over the molecule, a map shown in figure 11(d) could be obtained. Each pixel in the map corresponds to a time trace with an average of 100 switching events, giving a total of 75 000 switching events measured over the same molecule. These measurements were carried out in constant-current mode and thus the measured rate is directly proportional to the quantum yield of the switching process (number of switching events/number of tunneling electrons). It is clear that the switching rate in a given direction is asymmetric over the molecule. On the practical side, this difference can be exploited to control the direction of the tautomerization reaction. If the current is injected in a position where the probabilities for switching back and forth

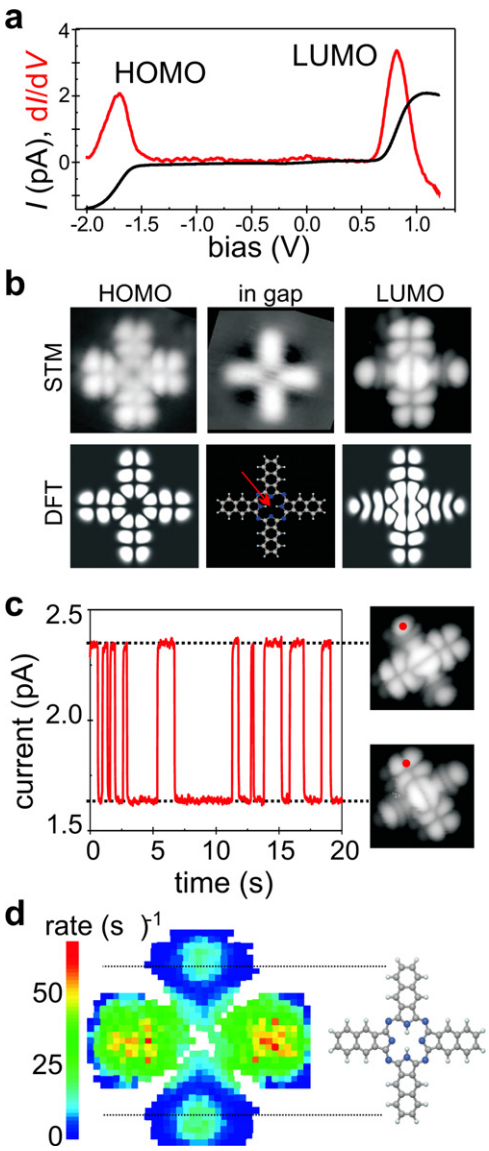

Figure 11. Molecular switches based on hydrogen tautomerization. (a) $\mathrm{d}I/\mathrm{d}V$ spectroscopy of naphthalocyanine showing resonances corresponding to the tunneling through the frontier molecular orbitals measured on an NaCl bilayer on Cu(111). (b) STM imaging at the biases corresponding to the resonances allows direct visualization of the symmetries of the molecular orbitals (top) and comparison with DFT calculations on isolated molecules (bottom). (c) Increasing the bias voltage causes the current to oscillate between two stable states. Orbital imaging can be used to investigate changes in the molecular orbitals due to the switching reaction. (d) Spatial dependence of the switching rate measured in the constant-current measurement. From [12]. Reprinted with permission from The American Association for the Advancement of Science.

are very different, the final position of the hydrogen atoms can be selected with a high probability (approx. 90%). The striking feature of the map shown in figure 11(d) is that the largest switching rate is achieved when the tip is above the far periphery of the molecule, i.e. >10 Å from the reaction site. This points to the importance of the increased lifetime of the tunneling electron on the molecule due to the presence of the insulating film and the relevance of vibronic excitation in the switching process.

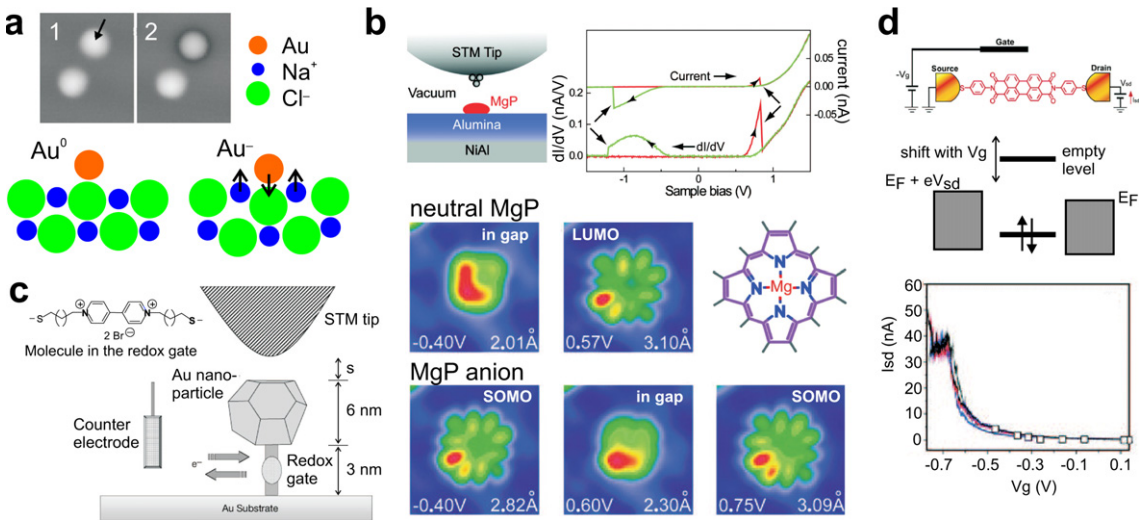

Figure 12. Examples of charge switching. (a) Top: a single gold atom deposited on an ultrathin NaCl insulating layer on a Cu(111) surface can be controllably switched between $z = 0$ (1) and $z = -1$ (2) charge states. Bottom: The charge on the gold atom is stabilized by a reorganization in the ionic thin film. From [13]. Reprinted with permission from The American Association for the Advancement of Science. (b) STM experiments on charge switching of a single magnesium porphine (MgP) deposited on an ultrathin alumina film on NiAl(110) surface. Top: IV- and $\mathrm{d}I/\mathrm{d}V$ curves showing hysteretic, bistable behavior. The positive and negative bias sweeps are indicated by red and green color, respectively, and the switching events are indicated by black arrows. Bottom: Switching is a result of electron addition to the LUMO. STM imaging shows how this results in a formation of a singly occupied molecular orbital (SOMO) that can be probed both at negative (electron removal from the SOMO) and positive (electron addition to the SOMO) bias. Adapted with permission from [14]. Copyright 2008 American Chemical Society. (c) Schematic of the experiment of Gittins *et al*: a redox-active molecule is sandwiched between a gold nanoparticle and a gold substrate and electrochemical STM was used to examine the electrical characteristics of this device. Electrons can be injected into the redox gate by applying a suitable potential on the substrate while the potential between the tip and the substrate (V_b) is controlled independently. Reprinted by permission from Macmillan Publishers Ltd: Nature [208], copyright (2000). (d) Top: a schematic of a single-molecule field effect transistor (FET) which consists of a redox molecule (perylene tetracarboxylic diimide) covalently bonded to a source and drain electrode and an electrochemical gate. Middle: By adjusting the gate voltage, the LUMO of the molecule shifts to within the bias window between the Fermi levels of the source and drain electrodes, resulting in a nearly three orders of magnitude increase in the source–drain current. Bottom: experimental results of the source–drain current as a function of the potential of the electrochemical gate. Adapted with permission from [210]. Copyright 2005 American Chemical Society.

What makes this molecular switch particularly attractive is that the conformational changes are confined to the center of the molecule and yet have an effect on the delocalized molecular orbitals over the entire molecule. This makes this molecule a promising candidate as a building block for more complicated molecular assemblies towards the goal of constructing molecular logic units. As a first step in that direction, the authors demonstrated that the switching processes can be coupled to neighboring molecules: charge injection in one molecule can induce tautomerization in an adjacent molecule [12].

4.3. Charge switching

Charge switching observed by STM. Before discussing molecular switches based on a redox reaction, we will consider the simplest type of charge switch as it demonstrates some of the basic concepts: a single atom. If the atom is directly adsorbed on a metal substrate, the strong coupling between the atomic orbitals and the electronic levels of the metal prevents permanent charging of the atom. However, if it is adsorbed on an ultrathin insulating film, the lifetime of the electron on the atom can be considerable increased. The question is if this can even lead to permanent charging. Typically, one would assume that the tunneling rates between the atom and the substrate are still too high and hence only transient charging would be possible. However, relaxation of the insulating layer can stabilize the charge on the atom and lower the ionization level below the Fermi level of the electrodes, leading to permanent charging. This is exactly the experiment described by Repp and co-workers (see figure 12(a)). They showed that Au atoms adsorbed on an ultrathin NaCl monolayer can be made permanently negatively charged [13]. The reorganization of the sodium and chloride ions of the insulator following the charge transfer to the Au atom stabilizes the new state and leads to a stable charged state, at low temperature. Subsequently, the same team demonstrated that, with Ag, three different charge states can be accessed (Ag^-, Ag^0 and Ag^+) [28]. These and other studies have demonstrated that this kind of process is general to atoms on polar insulating films [13, 28, 206].

Also molecular charge switching requires bistability of the charge states of the molecule. In the STM geometry, this can be achieved if (i) the lifetime of the tunneling electron on the molecule is sufficiently long and (ii) there is a mechanism that stabilizes the extra charge on the molecule [13, 14, 28]. One possibility for realizing this in practice is adsorbing the molecules on an ultrathin insulating film, in analogy to the Au and Ag atoms discussed above. The insulator reduces the tunneling coupling between the molecule and the substrate, and ionic reorganization in the film due to an added electron on

the molecule can stabilize the charge state. This approach has been demonstrated by the group of Ho, who studied charge switching of magnesium porphine adsorbed on an ultrathin alumina film on an NiAl(110) surface (see figure 12(b)) [14]. They demonstrated that the molecule can be controllably charged with one extra electron, and then uncharged by applying a negative bias potential in the STM. The added electron occupies the LUMO, resulting in the formation of a singly occupied molecular orbital (SOMO). This change can be detected by STM orbital imaging: in the case of an SOMO, the orbital images both at positive and negative bias are identical as they correspond to either the addition (positive bias) or removal (negative bias) of an electron to/from the same orbital. The relative stabilities were found to depend on the exact adsorption site within the complex unit cell of the alumina surface.

The use of diluted SAMs also offers the possibility to study intrinsic switching. In fact, it has proven very useful for qualitative studies on several types of switchable molecules. For example, Seo *et al* described conductance switching of thiol-tethered Ru(II)-terpyridine complexes embedded in alkanethiolate monolayers [207]. The authors observed that resonant transmission through the LUMO at positive bias resulted in permanent charging of the complex, which gave rise to hysteretic $I(V)$ curves. The charge could be reversibly taken off the molecule at negative bias.

Redox switching observed by electrochemical STM. There is an alternative approach to studying charge switching in single-molecule junctions compared to low temperature STM: electrochemical STM as discussed above. In the first study of this kind, Tao described experiments on Fe(III)-protoporphyrin [16]. The author showed how alignment of the LUMO of the molecule with the Fermi levels of the tip and the substrate changed the conductance by an order of magnitude and demonstrated efficient gating of the molecular charge state.

The work of Tao was followed by an influential paper by Gittins *et al* [208], who used STM to investigate electrochemically induced conductance switching in *N*,*N*-di-(10-mercaptodecyl)-4-4′-bipyridinium dibromide (bipy). The experiments were carried out in a gold nanocluster–bipy–substrate system, where an STM tip was used to contact the gold nanocluster (see figure 12(c)). STM experiments in the absence of electrochemical gating showed a single sharp resonance at negative bias, which the authors attributed to the tunneling through the $bipy^{\cdot+}$ state (the molecule is in the dication state at equilibrium). Gittins *et al* determined the decay length by measuring the dependence of the tunneling current on the tip height in an electrochemical STM and found that it decreased significantly upon reduction of the bipy molecules from $bipy^{2+}$ to $bipy^{\cdot+}$.

Subsequent experiments have used the STM break-junction (STM-BJ) technique. This method yields statistical information (histograms) on many molecular junctions formed sequentially (see above) [17, 21, 45, 47, 134, 209–211]. By carrying out STM-BJ experiments in an electrochemical STM, electrochemical gating can be used to adjust the Fermi levels of the tip and the substrate with respect to the molecular energy levels [17, 21, 209–212].

In the first report of this kind Haiss *et al* investigated changes in the conductivity of 6-[1′-(6-mercapto-hexyl)-[4,4′]bipyridinium]-hexane-1-thiol iodide (6V6) due to the applied electrochemical potential [17]. The molecules were not dissolved in solution, but already adsorbed on the surface during the tip–substrate contact. The authors were able to distinguish between one, two or three molecules being adsorbed in the tip–substrate junction and extracted a molecular conductivity of 0.49 nS, in line with previous experiments on molecules embedded in a self-assembled monolayer. Upon applying a potential on both the tip and the substrate with respect to a reference electrode in solution, they were able to modulate the molecular conductivity by a factor of six. The potential region, where the changes in the molecular conductivity occurred, corresponded to the known reduction potential of the bipyridinium moiety of 6V6 from V^{2+} to V^{+} [17]. Later experiments on molecules with different standard redox potentials further confirmed the effect of the electrochemical redox reaction on the molecular conductivity [211, 213].

The group of Wandlowski has also been active in using STM-BJ junctions under electrochemical control to study switching of bipyridinium and perylene bisimide derivatives [18, 136, 214, 215]. They carried out detailed investigations of both mono- and dithiol-derivatized molecules that allowed us to control the nature of the molecular junction: symmetric (dithiol) or asymmetric (monothiol). In the case of dithiol-derivatized bipyridinium, the STM break-junction technique yielded individual molecules bridging the tip and substrate gap. By tuning the potentials of the tip and the substrate with respect to a reference electrode (with a fixed small tip–substrate bias), the authors observed a sigmoidal increase in the molecular conductance that coincided with the known electrochemical formal potential of the $bipy^{2+}/bipy^{\cdot+}$ redox couple. This was attributed to the higher conjugation of the radical cation with respect to the dication. This observation is qualitatively similar to the results of Haiss *et al*; however, the saturation of the conductance past the reduction potential was more clearly observed [17, 18]. The authors attributed this to the strict absence of oxygen in their experiments as oxygen is known to react with dithiol-derivatized bipyridinium.

In the case of a monothiol monolayer pre-adsorbed on one of the electrodes, the authors focused in detail on the interpretation of the STM experiments based on electrochemical electron transfer theory [136, 215]. This yielded additional information on the mechanism of charge transport in such molecular junctions. The authors were able to show that switching can be understood within the physics of a weakly coupled quantum dot: the current is the sum of the contributions of the various molecular orbitals within the bias window.

Tao *et al* have described further measurements aimed at understanding details of transport in single-molecule junctions under electrochemical control (see figure 12(d)) [21, 209, 210]. They have investigated the effects of electrochemical charging (either reversible [21, 210] or irreversible [209]), electron donating side groups [209] and solvent/electrolyte [21]. In particular, they investigated electrochemical gating of perylene

tetracarboxylic diimide (PTCDI) and showed that electron addition due to the electrochemical gating results in a change of conductivity by three orders of magnitude [210]. Subsequent studies on three different PTCDI derivatives showed that the gate voltage had a significant effect on the temperature dependence of the molecular conductance. Below the onset of resonant tunneling through the LUMO orbital, the transport occurs via a thermally activated two-step process in aqueous solution. The activation energy of this process depended on the gate voltage and tended towards zero as the gate voltage was made more negative, i.e. the LUMO orbital was tuned within the bias voltage window. In contrast to an aqueous solution, the molecular conductance was temperature-independent in an organic solvent (toluene). This can be rationalized by considering the solvent reorganization energy in the Marcus model: the charge due to the added electron on the molecule does not couple to the non-polar solvent molecules and hence the solvent reorganization energy is very small in an organic solvent. All the PTCDI derivatives had overall similar qualitative behavior. However, as expected, the linkage chemistry had an effect on the actual values of conductance and, in addition, the sub-threshold slopes were found to be different for the different molecules. These studies show that it is possible to achieve transistor-type behavior and large switching ratios due to electrochemical charging in molecular junctions, in complete analogy to the solid-state three-terminal devices [19, 20]. At the same time, the environment (aqueous electrolyte) will have an effect on the observed response.

A report by Albrecht *et al* showed that it is also possible to carry out electrochemically gated transistor experiments on single molecules in ionic liquids [212]. They showed on/off ratios of 50 due to electrochemical reduction of an Os bisterpyridine complex in ionic liquid (1-butyl-3-methylimidazolium hexafluorophosphate). This study demonstrated the flexibility of the electrochemical control: by independently controlling the tip and substrate potentials with respect to the reference electrode it is possible to induce rectifying behavior as well [212].

Finally, Tsoi *et al* studied quinone-modified oligo(phenylene vinylene) molecules in an electrochemical STM set-up [216]. They demonstrated that the reversible switching of the molecule between reduced hydroquinone and oxidized quinone forms under electrochemical control resulted in significant changes in the molecular conductivity. Their analysis indicates that the high conductivity of the hydroquinone form is due to full bond conjugation throughout the molecule. In contrast, this conjugated path is broken in the quinone form of the molecule and hence the conductivity is lowered (see also [217]).

Charge switching in a device structure. There are only very few examples of charge switching in a molecular device geometry. Here, we mention the very recent work by Liao *et al* on TTF molecules [218]. They prepared very regular networks of gold nanoparticles (10 nm diameter) in which neighboring nanoparticle pairs are connected by one or a few TTF molecular bridges (see figures 7(c) and (d)). Indeed, Liao *et al* observed a significant conductance increase upon oxidizing the TTF molecular bridges in the network structure. Moreover, switching was demonstrated to be reversible.

Anticipating the next section, we note once again that redox reactions play a pivotal role in the switching process of mechanically interlocked molecules as well. Nevertheless, we deal with these molecules separately, since they are true conformational switches, in contrast to the molecules discussed in this section.

4.4. Mechanically interlocked switches

As the interlocked molecular switches have played a very prominent role in the history of switchable molecular devices, we discuss them in detail. J Fraser Stoddart has been the essential driving force behind the synthesis of mechanically interlocked molecules, such as ring-like catenanes and linear rotaxanes (see figure 3(b)) [7]. In these molecules, an outer ring can move between two stations on a macrocycle or molecular rod, respectively. If two different stations are chosen, e.g. one being a tetrathiafulvalene (TTF) unit and the other being a 1,5-dioxynaphthalene (DNP) unit, the ring will preferentially be located at the TTF unit. The situation in which the ring is located around the DNP station can be considered a metastable state. At the end of the last millennium, Stoddart joined forces with James Heath and Stanley Williams to create switchable devices based on mechanically interlocked molecules. The basic idea behind this effort was that the conductance of a device should change when the outer ring moves from one station to the other. An intuitive reason for this is that the extension of the frontier molecular orbitals and hence the overlap with the electrodes changes significantly between the two molecular co-conformers (for a more elaborate study, see [219]).

The first major result coming from the Heath–Williams–Stoddart collaboration was reported by Collier *et al* [187]. Three types of 'rotaxanes' were considered, all having the same symmetric dumbbell backbone containing two bipyridinium stations. For the first molecular type, $R(1)$, a single encircling crown ether ring was present. This ring can therefore hop between both bipyridinium stations, resulting in two degenerate molecular states. For $R(2)$, two encircling rings were present, i.e. one on each station, whereas $R(0)$ contained no ring at all. Devices were created by first patterning Al/Al_2O_3 wires on a silica substrate, followed by deposition of the molecules of interest as a Langmuir–Blodgett film. Subsequently, a 5 nm Ti layer and a 100 nm Al top layer were evaporated through a shadow mask by electron beam deposition. It is important to note that all of these devices incorporate PF_6^- counterions in addition to the switchable molecules. For the $R(1)$-based devices, Collier *et al* found irreversible conductance switching. As prepared, the devices turned out to be in the 'on' state. However, upon applying a voltage of 0.7 V or more (with respect to the grounded top contact), the devices turned off indefinitely. Although other control devices showed passive tunneling behavior, samples incorporating $R(0)$ and $R(2)$ molecules behaved similar to those incorporating $R(1)$ molecules. Hence, the switching mechanism was tentatively attributed to oxidation of the

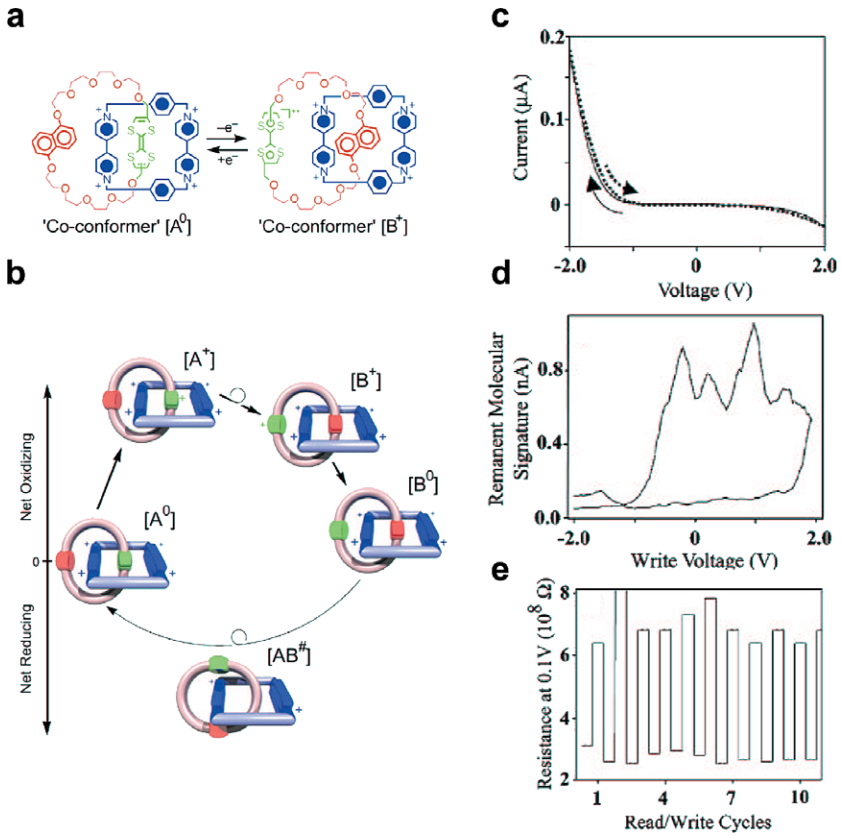

Figure 13. Conductance switching of a catenane-based molecular solid-state device by Collier *et al* [220]. (a) Two states of a [2]catenane molecule. The ground state is a co-conformer [A^0]. In this case, the TTF unit is located inside the cyclophane. (b) Proposed switching mechanism in the device. When the [2]catenane is oxidized (by applying a bias of −2 V), the TTF groups (green) are ionized, resulting in Coulomb repulsion with the tetracationic cyclophane (blue). This causes circumrotation of the ring, yielding state [B^+]. When the voltage is decreased to a near-zero bias, [B^0] is formed. Partial reduction of the cyclophane (at a 12 V bias) is necessary to regenerate [A^0]. The intermediate co-conformer [$AB^\#$] is indicated with an unknown oxidation state. (c) $I(V)$ hysteresis loop of one of the devices (stack: poly-Si/SiO_2/catenane monolayer/Ti/Al), at 291 K. The authors relate the asymmetry of the curve to the two different electrode materials. (d) The remnant molecular signature of the device, measured by varying the write voltage in 40 mV steps and by reading the device at −0.2 V (see the main text). (e) Switching operation of the device. The junction resistance was read at a bias of 0.1 V as the device was alternately opened at +2 V and closed at −2 V. The authors relate the 'off' state to [A^0] and the 'on' state to [B^0]. From [220]. Reprinted with permission from The American Association for the Advancement of Science.

dumbbell, rather than to mechanical shuttling of the crown ether ring (see section 4.3).

Next, the Heath and Stoddart groups focused on [2]catenane-based devices [220]. In figure 13(a), the chemical structure of the molecules used is shown schematically. On the larger crown ether ring, a TTF and a DNP unit are present. This ring itself is interlocked with a tetracationic cyclophane that includes two bipyridinium units (each 2+). As a result, these catenane molecules are bistable. The ground state co-conformer is the one in which the TTF unit is located inside the cyclophane (state [A^0]). In figure 13(b), the proposed redox-based mechanism of shuttling is schematically shown. The device structure that was chosen differed slightly from the 1999 work. In this case, the bottom electrode consisted of n-type polycrystalline Si with a 1–1.5 nm thick oxide layer, on top of which the molecular layer (including counterions) was deposited by the Langmuir–Blodgett technique. Just as for the 1999 devices, this resulted in relatively weak electronic coupling between the molecules and the bottom electrode. As a top electrode, a Ti/Al double layer was used, which was grounded in all experiments. Collier *et al* observed reversible conductance switching for these devices. In figure 13(c), we reproduce their current–voltage curves, where V_b was ramped back and forth between −2 and +2 V. A slight hysteresis between forward and backward scans can be seen, which could not be explained by capacitive effects. To study this effect in more depth, the authors determined the state of the device at low bias (0.1 V, 'reading') after the voltage had first been set by 'writing' at a larger bias. This so-called remnant molecular signature, shown in figure 13(d), exhibited two conductance states: 'on' and 'off'. Writing from 'on' to 'off' could be done using a positive voltage greater than 2 V, whereas resetting to the 'off' state could be done using a negative bias below −1.5 V. The authors found 'on'–'off' ratios of typically a factor of two, with large variations. Some devices could be cycled for a few hundred times over two months. In contrast to the 1999 paper on rotaxane devices, reversible switching in these catenanes was interpreted as a mechanical effect. One of the main arguments for this was the measured temperature dependence. It was seen that the on–off ratio of the device

decreases with decreasing temperature, becoming unity near 220 K. This observation is consistent with the fact that at least one of the transitions in the full switching cycle, i.e. the regeneration of the ground state [A^0] via the metastable state [$AB^{\#}$], is expected to be an activated step (see figure 13(b)).

The success of the papers discussed above triggered a larger scale effort by the groups involved. In 2001, devices made of monolayers of [2]catenanes, double-station [2]pseudo-rotaxanes and single-station [2]rotaxanes, respectively, were presented and compared [221]. A step in the direction of applications was set by Luo *et al* [188]. They reported rotaxane-based memory devices based on a cross-bar architecture and state-of-the-art lithographic techniques. For this, vertical devices with areas as small as 0.005 μm^2 were constructed. Another technologically interesting development was presented in 2003, when it was shown that working devices could be fabricated with a single-walled carbon nanotube as a bottom electrode [222]. In this way, the effective device area was minimized to 0.002 μm^2 or roughly 2000 catenane molecules. In the same year, the Williams group added to this by demonstrating vertical devices based on imprint lithography [223]. In contrast to the work by Luo *et al*, 'on'–'off' ratios as high as 10^4 were found.

An on-going issue in molecular electronics is the question if the effects observed are truly intrinsic to the molecules in the device. In 2003, a discussion on this matter materialized for switchable rotaxane- and catenane-based devices after a critical review in Science [224]. Specifically, the role of the electrodes was debated [36–38, 225, 226]. First, several groups demonstrated that switching with high 'on'–'off' ratios can be achieved in molecular devices that incorporate noble metals (Au, Ag, Pt) as bottom and/or top contacts [37, 39, 225]. Here, switching from 'off' to 'on', and vice versa, was connected to the formation and breakdown of metallic filaments under the influence of the applied potential. Indeed, the exact chemical content of the molecular layer appeared of minor importance for the functionality of these devices. A second matter of concern was the influence of the Ti layer, which serves as an adhesion layer between the molecules and the final top electrode (Al, Au, Pt). The choice of these materials follows common practice in thin film laboratories, but its advantages become less obvious in molecular devices. Not unexpectedly, it was shown that Ti reacts heavily with the organic molecules to form titanium carbide [36, 226]. For smaller molecules, this may lead to destruction of the organic layer. For larger molecules, this problem could be circumvented by allowing for a 'sacrificial' organic group at the top of the molecular layer. In addition to carbide formation, severe TiO_2 formation was reported for the case of oxidized bottom electrodes [226]. To counter these objections, Heath and Stoddart noted that in their devices the bottom contact consisted of either Al/Al_2O_3 or Si/SiO_2 or carbon nanotubes, so that filament formation from the bottom upwards is unlikely [187, 188, 220, 222]. In addition, they designed new experiments to investigate their exact device behavior in more detail [227–230]. Finding direct evidence for mechanical shuttling turned out to be experimentally difficult. Therefore, Flood *et al* chose to do indirect control experiments for double-station (TTF and DNP)

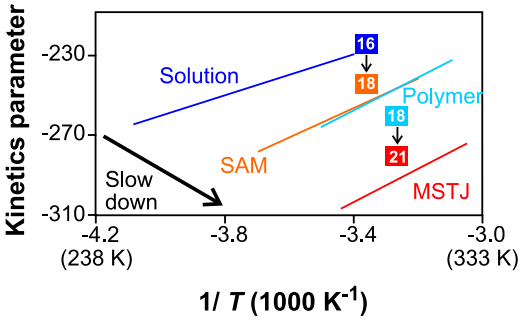

Figure 14. Study of the relaxation step in rotaxanes (see figure 3(b)) from the metastable 'on' state (ring positioned on the DNP) to the ground, 'off' state (ring positioned at the TTF) [227]. Four environments are compared, in which steric hindrance for molecular shuttling increases gradually: (i) molecules in solution; (ii) molecules in a polymer matrix; (iii) molecules in an SAM and (iv) molecules in a true vertical device. The kinetics of the rate-limiting step are plotted versus temperature in an Eyring plot. The difference in activation barrier is relatively small, going from 0.67 eV (or 16 kcal mol^{-1}, indicated) for a solution, to 0.76 eV (or 18 kcal mol^{-1}) for the SAM and polymer matrix, to 0.88 eV (or 21 kcal mol^{-1}) for the devices. This set of results provides indirect evidence that mechanical shuttling, though hindered, is taking place in the device geometry. From [227]. Reprinted with permission from The American Association for the Advancement of Science.

[2]rotaxanes and [2]catenanes. They focused on the relaxation from the metastable 'on' state, in which the ring is positioned on the DNP unit, to the ground state, in which it is around the TTF unit ('off' state). The authors performed temperature-dependent electrochemical experiments to characterize this activated step in detail. Four environments for the interlocked switch were compared, representing a series in which steric hindrance for molecular shuttling increases: (i) molecules in solution; (ii) molecules in a polymer matrix; (iii) molecules in a self-assembled monolayer, which can be seen as a half-device and (iv) molecules in a true vertical device. Figure 14 shows the kinetics of the rate-limiting step as a function of temperature. Clearly, there are large differences in the absolute timescales of the relaxation. Typically, the molecular devices switch back at a rate that is orders of magnitude slower than what is found for molecules in solution. Nevertheless, the authors pointed out that the difference in activation barrier is relatively small, going from 0.67 eV (or 16 kcal mol^{-1}) for the solution to 0.76 eV (or 18 kcal mol^{-1}) for the SAM and polymer matrix, to 0.88 eV (or 21 kcal mol^{-1}) for the devices. The continuous increase of these barriers was attributed to the steady decrease in mechanical freedom in these four systems. This result can hence be seen as indirect evidence for the fact that molecular shuttling, though hindered, is taking place in the molecular devices. The fact that the environment plays a direct role in mechanical switching of interlocked molecules was independently confirmed by Katz *et al* [231]. They showed that the shuttling rate of the activated step in an SAM made of (somewhat different) rotaxanes is dominated by the local friction. The latter quantity was varied by changing the viscosity of the liquid surrounding the SAM. A next control experiment focused on titanium carbide formation. DeIonno *et al* performed reflection–absorption infrared spectroscopy

on various Langmuir–Blodgett layers of rotaxanes before and after the evaporation of 2 nm of Ti [232]. With this technique, molecular vibrations (e.g. C–H stretching and ring bending) can be distinguished within the organic layer. DeIonno found that in less dense molecular layers (118 $Å^2$/molecule) the signature of such vibrations was lost after Ti evaporation, as a result of the formation of titanium carbide. The authors related this to the fact that rotaxanes in low-density layers are tilted at a relatively large angle with respect to the surface normal. Hence, Ti can easily penetrate into the central parts of the molecules, i.e. near the stations and encircling ring. For denser layers (73 and 54 $Å^2$/molecule, respectively), most molecular vibration peaks were still present after Ti evaporation. In other words, carbide formation appeared to be dominantly limited to the sacrificial endgroup of the molecule. Electric devices based on the same three-layer densities exhibited behavior consistent with the infrared data. The denser layers, for which the two stations and the surrounding ring are more shielded against Ti penetration, gave rise to switchable junctions. Devices built around the least dense layer of 118 $Å^2$/molecule, however, exhibited no conductance switching.

All in all, the work on rotaxane- and catenane-based devices has been of great importance to the field of molecular electronics. The pioneering efforts by the researchers involved represented one of the first fruitful collaborations of excellent synthetic chemists and physicists in molecular transport. The most important result of this collaboration is that molecular devices were created that exhibited reversible conductance switching over extended periods, with moderate 'on'–'off' ratios. Due to the high profile of the research, it is not surprising that a serious discussion started about the exact switching mechanism in these devices; a discussion which has not led to full consensus yet. Clearly, control experiments such as presented on interlocked switches in recent years are essential for a solid scientific basis of this research field.

4.5. Photochromic switches

Various types of photochromic molecules have been discovered and/or designed over the years, the archetypical examples being spiropyrane and stilbene [5, 6, 233–235]. Stilbene can be reversibly turned into dihydrophenanthrene upon illumination. Unfortunately, the latter product can irreversibly decay into phenanthrene in the presence of air, making stilbene a non-ideal candidate for devices [5, 233]. Nevertheless, the chemical research on stilbene has paved the path towards the synthesis of more stable photochromic switches, most notably the diarylethenes [5, 6, 234, 235]. Arguably, an even more famous group of photochromic molecules is formed by the azobenzenes [8, 10, 236, 237]. Most of the charge transport work has focused on these two groups of molecules. New photochromic switches, however, are continually proposed [238, 239]. As a result, light-sensitive molecular devices are likely to become more and more versatile and robust.

4.5.1. Azobenzenes. Azobenzenes undergo a *cis–trans* isomerization in solution upon illumination (see figure 3(a)).

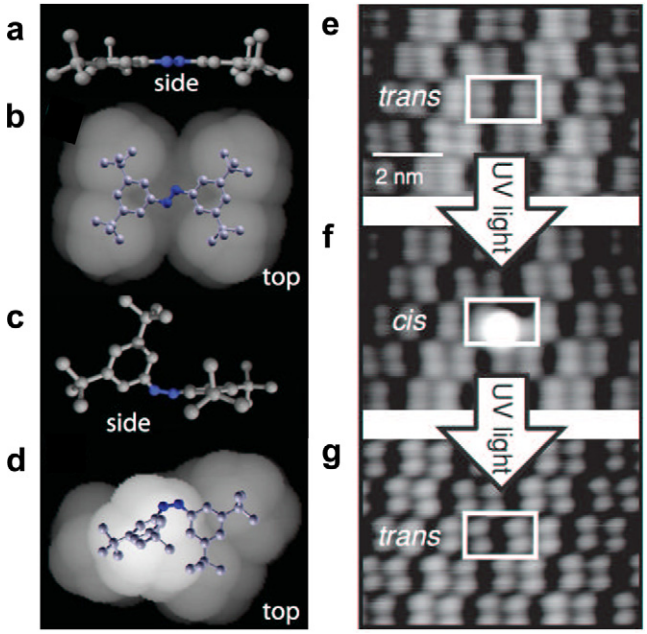

Figure 15. STM experiments on azobenzenes by the Crommie group. (a), (c) Calculated geometry of the four-legged tetra-tert-butyl-azobenzene (TTB-azobenzene) in the *trans*-form (a) and *cis*-form (c) of the molecule. The legs elevate the molecule from the surface, thus reducing molecule–metal interaction. (b), (d) Expected appearance of the *trans*-form (b) and *cis*-form (d) in an STM experiment, as calculated using density functional theory. (e)–(g) Reversible switching of an individual TTB-azobenzene molecule by sequential UV illumination, from *trans* to *cis* to *trans*. Reprinted with permission from [10]. Copyright (2007) by the American Physical Society.

However, it is not *a priori* clear that the same processes will occur after connecting the molecules to a metal. The presence of the substrate can affect photoswitching through a number of factors, two of the most important being quenching of the excited state and steric hindrance. To start with the latter, steric hindrance presents a fundamental limitation to the applicability of azobenzenes in two-terminal devices. Once a molecule is contacted, the distance between both electrodes is, in principle, fixed. A large change in the effective length of the molecule upon switching, as exhibited by azobenzenes, is therefore not easily accommodated. A scanning probe, on the other hand, does have the freedom to adapt to the state of the molecule. For this reason, most of the work on azobenzenes has been performed by STM.

Let us first discuss STM work on azobenzenes lying flat on a surface. In this configuration, the coupling between substrate and molecule is quite large. Indeed, the Crommie group showed that simple azobenzenes adsorbed on Au(111) do not exhibit photoswitching [10]. Therefore, they decided to increase the distance between the molecule and the surface by introducing four 'legs', i.e. tert-butyl side groups, on the benzene rings (see figures 15(a) and (c)). This physically lifts the molecule up from the surface. For these decoupled molecules, photoinduced isomerization was indeed demonstrated. In the experiment shown in figures 15(e)–(g), an individual *trans*-molecule is switched to the *cis*-state by

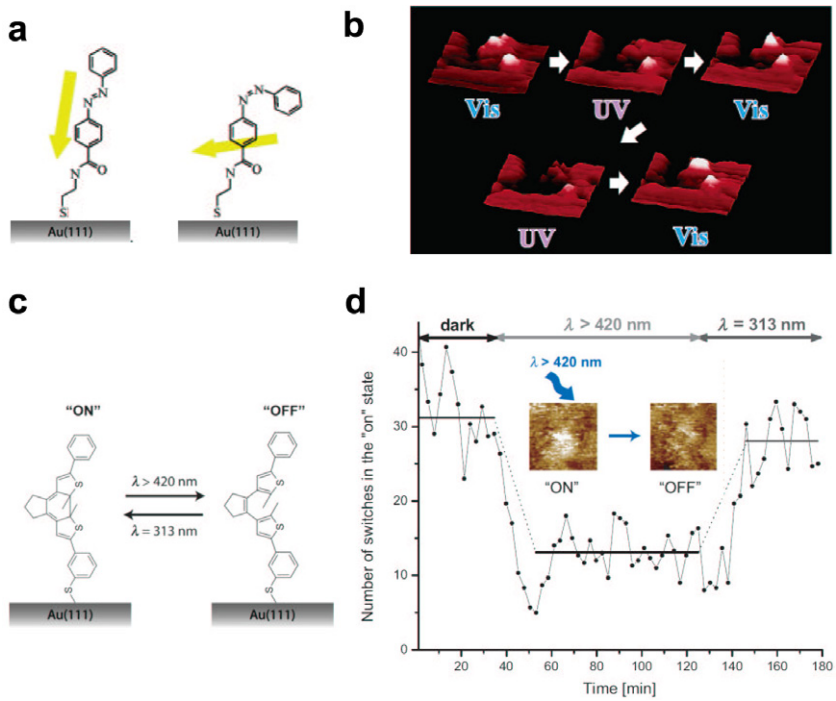

Figure 16. STM experiments on photochromic switches diluted in a SAM of dodecanemonothiols (see figure 5(c)). (a) *Trans*- and *cis*-form of a thiolated azobenzene coupled to Au(111) via a short alkane spacer. (b) Photochromic switching of an individual azobenzene molecule as a result of alternate illumination by visible and UV light. Reprinted with permission from [103]. Copyright 2003 American Chemical Society. (c) Closed and open states of a thiolated diarylethene. (d) Inset: single switching event (closed to open) of an individual diarylethene. Larger graph: statistical analysis of switching events in a larger area during subsequent illumination with visible light and UV light. The variations are due to stochastic switching (see figure 8). Note that for azobenzenes, the change in apparent height is dominated by a change in physical height, whereas for the diarylethenes, it is mostly a result of a change in conjugation (see (c)). From [105]. Reprinted with permission from Wiley.

UV light. After a second exposure to UV light, the molecule switches back to the *trans*-form. The difference in appearance between *cis*- and *trans*-forms, as found experimentally, was confirmed by calculations based on density functional theory (figures 15(b) and (d)). Interestingly, the Crommie group found that both UV and visible light induce switching with similar rates, contrary to what is seen for molecules in solution [10, 11]. Hence, the proximity of a metal still has a significant influence on the isomerization dynamics. Further STM experiments performed on flat-lying azobenzene derivatives emphasize both the versatility and complexity of molecular systems. In fact, it was shown that azobenzene isomerization can also be induced electrically by inelastic tunneling [9]. The inelastic tunneling mechanism involves sequential vibrational excitation of the molecule to overcome the isomerization activation energy barrier. However, the direction of the switching reaction could not be controlled [9]. In 2006, Grill and co-workers reported azobenzene switching by the electric field set-up by the STM tip [8]. More recently, they gave a fascinating example of how molecular switching can be influenced by the supporting surface [240]. For specific monolayers of *trans*-azobenzene derivatives on Au(111), they found that some molecules are switched to *cis* much more easily than others. Remarkably, the molecules that can be converted are found in a pattern that is spatially periodic. In other words, a very regular arrangement of addressable molecular switches is imposed onto the molecular layer by the Au(111) lattice, even though the monolayer itself is homogeneous. We end this paragraph with another exciting example of how the proximity of a metal can influence switching. Recently, Wolf and Tegeder demonstrated molecular switching of tetra-tert-butyl-azobenzene on Au(111) induced by a substrate-mediated charge transfer process [237]. In their picture, light-induced hot holes in the gold first move to the top of the d-band. After this, they transfer to the HOMO of the contacted azobenzene and initiate the switching process. This represents a captivating case of a switching mechanism that actually arises from the presence of a metal.

We now move to STM studies on azobenzenes that are connected to a substrate at one point only. This geometry can be seen as a half-device, where the STM tip plays the role of a remote second electrode. Inspired by the Weiss group, Yasuda *et al* studied molecular switching in a diluted SAM consisting of azobenzene-type molecules located in a matrix of dodecanethiols [103]. To prevent functionality loss, the authors chose to connect the azobenzenes to an Au(111) substrate by a short alkane spacer (see figure 16(a)). The individual azobenzene molecules were imaged as bright protrusions, i.e. their apparent height, h_{app}, was larger than that of the alkanethiols (see figure 5(c)). Upon illumination by UV light, however, these protrusions became significantly lower, one by one. These changes could be reversed by irradiation with visible light, as shown in figure 16(b). Since the *trans*-form of the azobenzene molecules has a larger

physical length, this result is consistent with *trans*-to-*cis* switching (visible light) and *cis*-to-*trans* switching (UV), respectively. In addition to light-induced switching the authors reported an extrinsic switching effect, which occurred quite randomly when scans were made at positive biases, again highlighting the need to distinguish between these two switching mechanisms. A contribution was also made by the Weiss group [241]. They studied azobenzene molecules with relatively long saturated chains, assembled in a decanethiol SAM. Light-induced switching was indeed observed with a more than 90% efficiency from *trans* (large h_{app}) to *cis* (smaller h_{app}). Reverse switching was also observed, although not for all molecules.

As mentioned above, switching azobenzene within a two-terminal device is not trivial. One way out would be to use very flexible electrodes. Del Valle *et al* argue that nanotubes or, if necessary, telescopic nanotubes should be able to accommodate the conformational change exhibited by switching azobenzenes [236]. Therefore, they calculated the conductance change for azobenzenes contacted by two carbon nanotubes. Not only did they find a considerable on–off conductance ratio, they also made the prediction that this ratio depends on the exact chirality of the nanotubes used. (We note that a similar effect has recently been predicted for diarylethenes [242].) To our knowledge, single-molecule measurements such as proposed by Del Valle *et al* are still to be performed. However, for complete azobenzene SAMs, a few experiments have been reported. First, Mativetsky *et al* used a conducting AFM set-up to create a quasi-two-terminal device (gold substrate–azobenzene SAM–metal-coated tip) with sufficient flexibility to adapt to the anticipated height change of the SAM [243]. Their study focused on UV-induced switching from the *trans*- to the *cis*-state. After illumination, they observed an increase of the conductance typically of a factor 25–30, which was explained to first order from the corresponding decrease in tunnel barrier length (SAM-height). A similar result was obtained using an Hg-droplet top electrode. In this case, the authors observed reversible conductance switching with a ratio around 25 [244]. Interestingly, upon switching from the *cis*- to the *trans*-form, the azobenzene molecules were able to lift the Hg droplet. The ability of azobenzene molecules to perform work establishes a connection to the growing research field on (photochromic) synthetic molecular motors and machines [245–250].

4.5.2. Diarylethenes. Diarylethenes (or rather dithienylethenes) were first synthesized by Irie *et al* [5]. Generally, they can be converted from a conjugated 'on' state to a cross-conjugated 'off' state upon illumination with visible light. The reverse process is possible with ultraviolet (UV) light (see figure 3(d)). The energy barrier between both isomers is typically much higher than for azobenzenes. Hence, diarylethenes cannot easily be switched by heating. Diarylethenes have a number of properties that make them attractive as molecular switches. For example, the photoisomerization reaction does not have significant side reactions and hence photodegradation is not as serious a problem as for many other photochromic switches [5]. Furthermore, their length change upon isomerization is negligible, making them well suited for two-terminal molecular devices. An impressive amount of research has been performed to characterize ensembles of diarylethene molecules, both in solution and in thin films [5, 252–256]. In particular, the work of Matsuda and Irie, and Fraysse *et al* paved the road for later research on conductance switching [252, 253]. The first group grafted two nitronyl nitroxides at both ends of a diarylethene molecule. Subsequently, they observed a large increase in the ferromagnetic coupling between both endgroups when the diarylethene spacers were switched from 'off' to 'on'. Fraysse *et al* investigated intramolecular charge transfer between two Ru-complexes coupled at each end of a diarylethene by both experimental and theoretical methods. These experiments suggested the feasibility of using diarylethenes for molecular memory devices with on–off ratios ∼50.

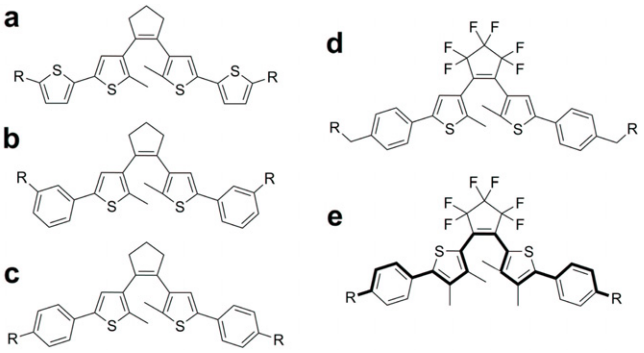

Figure 17. A set of diarylethenes that have been studied after connection to gold [104, 105, 117, 135, 175, 177, 251]. They differ mainly in their endgroups: (a) thiophene ring and thiol endgroup [117]; (b) phenyl endgroup with thiol(s) in meta-position [105, 177, 251]; (c) phenyl endgroup with thiol in para-position [251]; (d) phenyl ring with alkanethiol spacer in para-position. The middle ring in this molecule has been fully fluorinated for enhanced stability [135] and (e) fluorinated diarylethene switch which is linearly conjugated in the open state (indicated by the bold line), in contrast to (a)–(d). The closed state is cross-conjugated [175]. We note that molecules (b)–(d) can be reversibly switched after connection to gold, whereas the molecule in (a) can only be switched in one direction, from 'on' to 'off'. This series emphasizes the subtle influence of metal–molecule coupling on switchability. Note that all these molecules can be synthesized in a monothiol and a dithiol variety (R=H, R=SH or R=S-acetyl).

The first study that focused on conductance switching of diarylethenes contacted by a metal was presented by Dulić *et al* [117]. They investigated diarylethenes with thiophene endgroups (see figure 17(a)) contacted to gold through the Au–S bond. For this, they employed two different techniques. First, they explored photochromic conductance switching in break junctions (lithographic MCBJs). The conductance decreased by two orders of magnitude upon illuminating the molecular junctions with visible light, indicating switching of the molecules to the 'off' state. However, it proved impossible to switch the molecules back to the 'on' state. To check the generality of this conclusion, a second experiment was set up with the monothiol variety of the same molecules. In this case, diarylethene molecules were grafted on gold nanoparticles

(diameter ∼3 nm). Subsequently, optical absorption (UV–vis) spectroscopy was used to characterize the switching process. Whereas reversible photochromic switching was observed for molecules in solution, the situation was dramatically different for molecules connected to gold particles. In that case, switching was only possible from the 'on' to the 'off' state, in agreement with the break-junction experiments. In addition to these measurements, a series of ultrafast spectroscopy experiments (pump–probe) were performed by Hania *et al* [257]. Such experiments allow one to follow the switching process quantitatively on the sub-picosecond level. Indeed, measurements on diarylethenes (see figure 17(a)) connected to gold nanoparticles showed a strongly enhanced, bi-exponential decay of the excited state (timescales: 0.3 and 3 ps). This result indicated strong mixing of electronic states after covalent attachment of the molecule to the gold. In a fourth experiment, the same types of diarylethenes were investigated by STM (see figure 17(a)) [104]. For this, a diluted SAM of diarylethene-monothiols in a dodecanethiol matrix was created (cf Yasuda *et al* [103]). The authors demonstrated that the apparent height, h_{app}, of 'on'-state molecules decreases significantly upon illumination with visible light. Hence, individual switching events from 'on' to 'off' could be observed. However, light-induced switching from 'off' to 'on' was not observed, which is consistent with the two experiments described above. This study also proposed a statistical analysis method to convincingly separate intrinsic (light-induced) from extrinsic ('stochastic') switching [104] (see also [106]).

The four experiments discussed above presented a clear example of the influence of metal–molecule coupling on functionality. As a result, they triggered a significant number of theoretical studies on the details of the switching mechanism and on the conductance properties of diarylethenes connected to gold [258–265]. In particular, the contributions by Li *et al* dealt with the question why these molecules exhibited one-way switching only after connection to gold [258, 259, 261, 265]. It was shown that the HOMO of the open form ('off') is much more strongly coupled to the gold orbitals than the HOMO of the closed ('on') form. Hence, after the open state is photo-excited, the resulting hole in the HOMO level is immediately filled up by an electron coming from the gold, thus quenching the photoswitching process. For the closed form, this effect is much less dramatic, leading to one-way switching[10]. In other words, the strong electronic interaction between molecule and metal seriously hampers the switching process. A logical way out is to decrease this interaction by using non-conjugated spacer groups between molecule and electrode. This approach was taken by the Lindsay group who inserted a methyl spacer between the thiol group and the diarylethene central unit (see figure 17(d)). They employed the STM break-junction technique to find that the conductance of closed-state molecules is approximately two orders of magnitude larger than that of open-state molecules. These results were consistent with the on–off ratio found by Dulić *et al*[11] and with calculations (see figures 18(a) and (b)). Furthermore, the Lindsay group employed optical spectroscopy to independently demonstrate reversible switching of their diarylethenes on a thin gold surface. Unfortunately, an alkane spacer introduces an extra barrier for electron transport. Therefore, the Groningen research groups chose a different path. They first replaced the thiophene groups of the molecules used by Dulić by phenyls [266]. Subsequently, the thiol anchors were positioned at the meta-position of the phenyl rings, where the wavefunction of the HOMO has a node [259, 267] (see figure 17(b)). In this way, only minor overlap between molecular and electrode orbitals was assured. To test if this would yield reversible switching, Kudernac *et al* attached these molecules to gold nanoparticles and performed optical spectroscopy (UV–vis) [251]. Indeed, reversible photoisomerization was observed (see also [234]). Kudernac *et al* also investigated the case where the thiol is placed at the para-position of the phenyl ring (see figure 17(c)). Remarkably, this type of molecule exhibits reversible switching on gold as well. Although this unexpected result has been related to the tilt angle of the phenyl with respect to the central molecular unit [265], a full picture remains to be developed.

As a next step, Katsonis *et al* employed the diluted SAM method once more. They investigated photochromic switching of diarylethenes connected to Au via a thiol in the meta-phenyl position (see figure 17(b)) [105]. Indeed, they did observe reversible photochromic switching of individual molecules. To check the generality of the observed effect, they performed a statistical analysis on a set of individual diarylethenes located in the SAM, as shown in figures 16(c) and (d). Interestingly, around 30% of the molecules were not influenced by illumination, possibly as a result of local steric hindrance. The results obtained for individual molecules by STM were confirmed for the ensemble by UV–vis absorption spectroscopy experiments on semitransparent gold substrates [105].

The work in Japan, the US and the Netherlands triggered a new effort to create switchable devices based on diarylethenes. Various strategies were chosen to enhance room temperature stability[12]. For this, several groups chose to use intermediates to bridge the gap between the molecules and larger electrodes (see figures 7(a)–(d)). The Nuckolls group trapped fluorinated diarylethene molecules inside the gap of etched carbon nanotubes [164]. This type of device has great promise due to its small size and the possibility of integrating a gate electrode. Interestingly, they did observe photoswitching from the open to the closed state by UV light, while the reverse process could not be induced by illumination (see figure 18(c)). The authors relate this to energy transfer of the excited state of the closed molecule to the extended π-electron system, i.e. the nanotube. Remarkably, their result is exactly the opposite of the first work

[10] Interestingly, the mechanism proposed by Speyer and Ernzerhof *et al* for diarylethenes on gold differs strongly from the picture for azobenzenes by Wolf and Tegeder. In the first case, switching from off to on is hampered by hole transfer to the Au d-band (only for the 'off'-state molecule). In the second model, it is the reverse transfer from photon-induced holes from the Au d-band to the molecule that actually induces the switching of the molecule!

[11] Due to the difference in endgroups, the on–off ratio is the best quantity to use for a comparison. As expected, the 'on'-state conductance is lower for the molecules studied by Lindsay.

[12] We note that going to lower temperatures does bring enhanced stability, but hampers the switching from closed to open. For the latter a barrier has to be overcome by thermal activation, after photo-excitation [30].

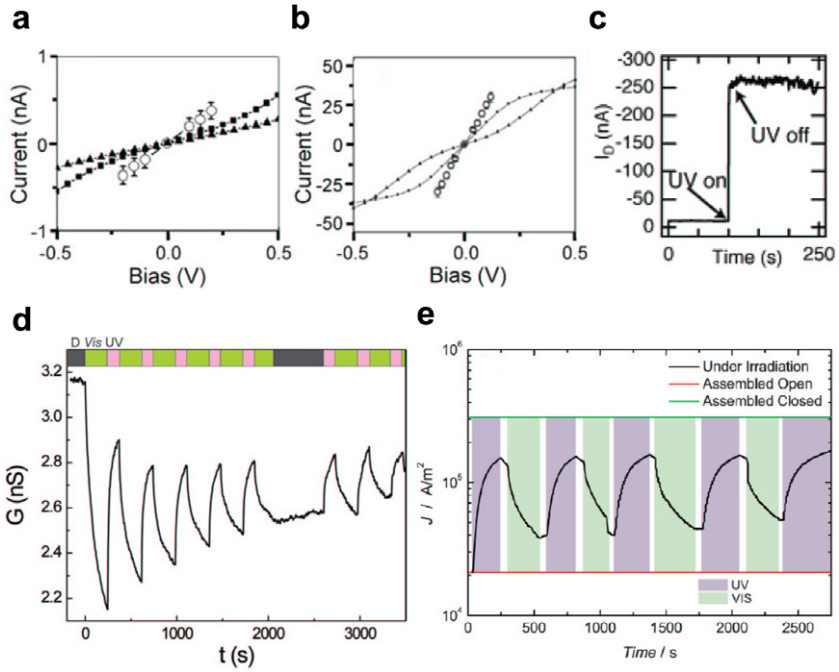

Figure 18. Conductance measurements on diarylethenes by various methods. (a), (b) Experimental (open circles) and calculated (closed symbols) current–voltage characteristics for open (a) and closed (b) diarylethene molecules. The diarylethene molecule used is depicted in figure 17(d) with R=SH, i.e. it is in the dithiolated form. Contacting was done by the STM-break-junction method; the current values represent a statistical average over many junctions, measured at a given bias. The calculations were done for molecules attached to hollow sites (triangles) and on-top sites (squares). Reprinted with permission from [135]. Copyright (2005) by the Institute of Physics. (c) Light-induced off-to-on switching of a diarylethene molecule connected inside the gap of a carbon nanotube (see figure 7(a)). Upon UV illumination, a 25-fold increase in conductance takes place. Switching from 'on' (closed form) to 'off' (open) turned out to be impossible in this geometry. The bias applied is −50 mV. Reprinted with permission from [164]. Copyright 2007 American Chemical Society. (d) Reversible conductance (G) switching for diarylethene molecules (see figure 17(b)) connected within a regular 2D network of nanoparticles (see figure 7(c)). Initially, the sample was in the dark (D). Then alternate illumination was performed with visible (vis) and UV light. For $2095 < t < 2650$, the sample was in the dark as well. Note the relatively low on–off ratio. This is a result of the limited number of molecules that are switched during the illumination times chosen, in combination with the percolative nature of the 2D network. This contrasts with the case of break junctions or SAM-based devices (parallel molecules). Reprinted with permission from [177]. Copyright 2009 American Chemical Society. (e) Reversible conductance switching for diarylethenes (see figure 17(b)) in an SAM device with a PEDOT:PSS top electrode (see figure 7(f)). Alternate illumination by UV and visible (vis) light is performed. Note that these authors plot current density. From [191]. Reprinted with permission from Wiley.

on diarylethenes on gold, which again stresses the importance of the details of the molecule–electrode coupling. We note that a different, pyrrole-form of the diarylethenes could be switched back thermally. The Nuckolls group found on–off ratios of around 25.

An alternative strategy is to use metal nanoparticles as intermediates. Since nanoparticles had already been used to test the functionality of molecules connected to a metal [117, 251], it was a logical step to use the same units to create a device. Two sets of such experiments have been performed, although they differ considerably in the exact approach. The Irie group synthesized relatively small gold nanoparticles first (3–6 nm diameter) [174, 175]. Next, these particles were allowed to react with several types of dithiolated diarylethenes, after which a droplet of the solution was placed onto a substrate with (interdigitated) gold electrodes. Although the resulting nanoparticle network was not very regular, it did establish a stable electrical connection between the larger electrodes. Moreover, Irie *et al* demonstrated reversible conductance switching by illumination. To complete their analysis, the authors also performed a charming test experiment. They synthesized a diarylethene switch, which is linearly conjugated ('on') in the open form and cross-conjugated in the closed form (see figure 17(e)). Indeed, a resistance increase was observed upon switching from open to closed.

A somewhat different approach was taken by Van der Molen *et al* [177]. They inserted dithiolated diarylethenes (meta-phenyl endgroups, see figure 17(b)) as bridges into a very regular monolayer of gold nanoparticles with a diameter of 10 nm (see figures 7(c) and (d)) [166, 171, 172]. Reversible conductance switching was indeed established in these percolative structures (see figure 18(d)). Nevertheless, photodegradation under UV light was also observed, leading to device deterioration after typically 10 switching cycles. A very important advantage of molecule–nanoparticle networks is that they allow for optical control experiments [172, 174]. In figure 19, it is shown how the surface plasmon resonance of the gold nanoparticles toggles between two positions as the molecules are switched between two conductance states. The resonance shift is due to the difference in dielectric constant ϵ of the two isomers. Figure 19 establishes a direct connection

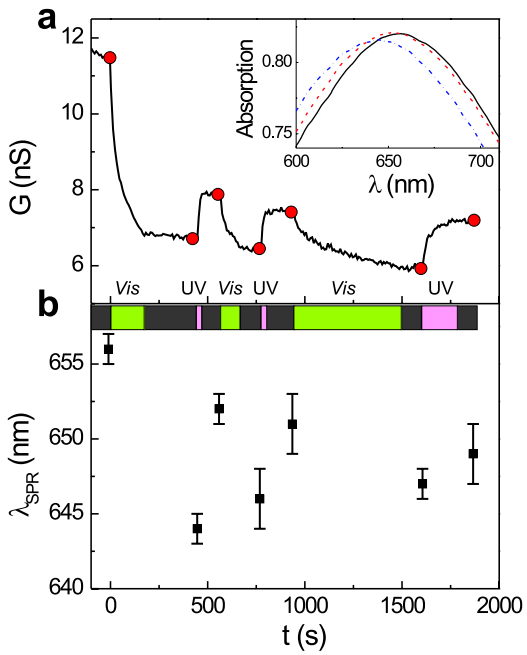

Figure 19. Independent confirmation of molecular switching by optical absorption spectroscopy. A nanoparticle network device (see figure 7(c)) with dithiolated diarylethene bridges (see figure 17(b)) is used. (a) Conductance switching as a result of UV and visible (vis) illumination. The gray areas indicate the intervals during which the sample was in the dark. At the end of such a period (red dots), a UV–vis optical absorption spectrum was taken (see inset for the first three curves). Upon switching the molecules from 'on' (higher permittivity ϵ) to 'off' (lower ϵ), the gold surface plasmon peak first shifts to lower wavelengths. (b) Position of the surface plasmon peak taken from the sequential absorption measurements. There is a direct correlation between conductance values and optical spectra. Reprinted with permission from [177]. Copyright 2009 American Chemical Society.

between conductance values and surface plasmon resonance position, providing two independent experiments in parallel.

Recently, diarylethenes have also been applied in devices based on SAMs [191, 268]. Kronemeijer *et al* created structures consisting of gold, a diarylethene SAM and a polymer (PEDOT:PSS) top electrode. The molecule they used was of the meta-phenyl type (see figure 17(b)). Kronemeijer demonstrated a room temperature conductance switch with an on–off ratio of about an order of magnitude (see figure 18(e)). Since the active molecules are protected from the ambient, these devices proved very stable. This work forms another beautiful example of how bottom-up research and top-down technology can result in completely new devices. Summarizing, the diarylethenes have proven to be a fascinating system for molecular electronics (and photochemistry), with high potential for future fundamental and applied research.

5. Conclusions and outlook

Over the past 15 years, quantitative charge transport experiments on switchable molecules have become possible. Reviewing the progress in the field, one finds that the basic philosophy of molecular electronics does indeed work: the required functionality of a device can be encoded into a molecule by chemical synthesis. In fact, switchable devices based on intrinsic molecular switches can be created that still operate at room temperature. However, it is not *a priori* clear if connecting a switchable molecule to electrodes will indeed lead to a switchable molecular device. In fact, in many cases it will not. Knowledge of the electronic and mechanical interactions between molecule and metal hence forms an essential ingredient in understanding molecular junctions. This is further illustrated by one of the biggest surprises of the field: extrinsic switching. Molecules that are passive, i.e. not designed to be molecular switches, can also exhibit stable, repeatable switching behavior in two-terminal devices. There are various examples of such 'extrinsic' switching and it is not obvious at the moment whether future applications of molecular switches will use extrinsic or intrinsic switching.

This research field is moving in the direction of a more quantitative understanding of the physical principles that govern—both intrinsic and extrinsic—molecular switching. Nevertheless, there are still many open questions in this area of nanoscience. A general understanding of functional metal–molecule–metal junctions will require insight from both theory and experiment. First of all, accurate first-principles calculations on the full metal–molecule–metal system are needed. Second, structural characterization down to the atomic scale is necessary to bridge the gap between theory and experiment. Recent advances in scanning probe techniques demonstrating single-charge detection with atomic spatial resolution, probing molecular orbitals in real space and atomic resolution imaging of organic molecules should be applied to these systems [78, 269, 270]. Third, much can be learnt from experiments on the switching dynamics of molecules attached to metals (e.g. to nanoparticles). Ultrafast pump–probe spectroscopy will allow new insights in the mechanisms that take place in the sub-ps time domain, yielding valuable information on the relevant potential energy surfaces. Finally, accurate transport measurement and IETS experiments, probing electron–phonon coupling, can be performed by break-junction techniques. Information on molecular vibration energies will form an essential ingredient in quantitative studies on the energetics of molecular switching. Developing a fundamental understanding of the actual switching mechanism in switchable molecular devices will be the key challenge in this field.

Acknowledgments

This work was financed by NWO/Chemical Sciences (PL, Vidi-grant 700.56.423) and by a NanoSci-E+ network grant in the European Research Area (SJvdM). We thank Amar Flood, Constant Guédon, Marius Trouwborst and Tibor Kudernac for carefully reading this manuscript.

References

[1] Mann B and Kuhn H 1971 *J. Appl. Phys.* **42** 4398
[2] Aviram A and Ratner M A 1974 *Chem. Phys. Lett.* **29** 277
[3] Metzger R M 2008 *J. Mater. Chem.* **18** 4364

[4] Feringa B L 2001 *Molecular Switches* (Weinheim: Wiley–VCH)
[5] Irie M 2000 *Chem. Rev.* **100** 1685
[6] Weibel N, Grunder S and Mayor M 2007 *Org. Biomol. Chem.* **5** 2343
[7] Stoddart J F and Colquhoun H M 2008 *Tetrahedron* **64** 8231
[8] Alemani M, Peters M V, Hecht S, Rieder K-H, Moresco F and Grill L 2006 *J. Am. Chem. Soc.* **128** 14446
[9] Choi B Y, Kahng S J, Kim S, Kim H, Kim H W, Song Y J, Ihm J and Kuk Y 2006 *Phys. Rev. Lett.* **96** 156106
[10] Comstock M J *et al* 2007 *Phys. Rev. Lett.* **99** 038301
[11] Comstock M J, Levy N, Cho J, Berbil-Bautista L, Crommie M F, Poulsen D A and Frechet J M J 2008 *Appl. Phys. Lett.* **92** 123107
[12] Liljeroth P, Repp J and Meyer G 2007 *Science* **317** 1203
[13] Repp J, Meyer G, Olsson F E and Persson M 2004 *Science* **305** 493
[14] Wu S W, Ogawa N, Nazin G V and Ho W 2008 *J. Phys. Chem.* C **112** 5241
[15] Meded V, Bagrets A, Arnold A and Evers F 2009 *Small* **5** 2218
[16] Tao N J 1996 *Phys. Rev. Lett.* **76** 4066
[17] Haiss W, van Zalinge H, Higgins S J, Bethell D, Hobenreich H, Schiffrin D J and Nichols R J 2003 *J. Am. Chem. Soc.* **125** 15294
[18] Li Z, Han B, Meszaros G, Pobelov I, Wandlowski T, Blaszczyk A and Mayor M 2006 *Faraday Discuss.* **131** 121
[19] Osorio E A, O'Neill K, Wegewijs M, Stuhr-Hansen N, Paaske J, Bjørnholm T and van der Zant H S J 2007 *Nano Lett.* **7** 3336
[20] Osorio E A, O'Neill K, Stuhr-Hansen N, Nielsen O F, Bjørnholm T and van der Zant H S J 2007 *Adv. Mater.* **19** 281
[21] Li X L, Hihath J, Chen F, Masuda T, Zang L and Tao N J 2007 *J. Am. Chem. Soc.* **129** 11535
[22] Hipps K and Mazur U 2002 *Handbook of Vibrational Spectroscopy* (Chichester: Wiley) chapter (Inelastic Electron Tunneling Spectroscopy)
[23] Agraït N, Yeyati A L and van Ruitenbeek J M 2003 *Phys. Rep.* **377** 81 and references therein
[24] Smit R H M, Noat Y, Untiedt C, Lang N D, van Hemert M C and van Ruitenbeek J M 2002 *Nature* **419** 906
[25] Eigler D M, Lutz C P and Rudge W E 1991 *Nature* **352** 600
[26] Qiu X H, Nazin G V and Ho W 2004 *Phys. Rev. Lett.* **93** 196806
[27] Thijssen J M and van der Zant H S J 2008 *Phys. Status Solidi* **245** 1455
[28] Olsson F E, Paavilainen S, Persson M, Repp J and Meyer G 2007 *Phys. Rev. Lett.* **98** 176803
[29] Grunder S, Huber R, Horhoiu V, Gonzalez M T, Schönenberger C, Calame M and Mayor M 2007 *J. Org. Chem.* **72** 8337
[30] Dulić D, Kudernac T, Puzys A, Feringa B L and van Wees B J 2007 *Adv. Mater.* **19** 2898
[31] Gutlich P, Hauser A and Spiering H 1994 *Angew. Chem. Int. Edn* **33** 2024
[32] Salitros I, Madhu N T, Boca R, Pavlik J and Ruben M 2009 *Mon. Chem.* **140** 695
[33] Gamez P, Sanchez Costa J, Quesada M and Aromi G 2009 *Dalton Trans.* **38** 7845
[34] Osorio E A, Moth-Poulsen K, van der Zant H S J, Paaske J, Hedegård P, Flensberg K, Bendix J and Bjørnholm T 2010 *Nano Lett.* **10** 105
[35] Förster T 1948 *Ann. Phys.* **437** 55
[36] de Boer B, Frank M M, Chabal Y J, Jiang W, Garfunkel E and Bao Z 2004 *Langmuir* **20** 1539
[37] Stewart D R, Ohlberg D A A, Beck P A, Chen Y, Williams R S, Jeppesen J O, Nielsen K A and Stoddart J F 2004 *Nano Lett.* **4** 133
[38] Haick H, Ghabboun J and Cahen D 2005 *Appl. Phys. Lett.* **86** 042113
[39] Beebe J M and Kushmerick J G 2007 *Appl. Phys. Lett.* **90** 083117
[40] Datta S 1995 *Electronic Transport in Mesoscopic Systems* (Cambridge: Cambridge University Press)
[41] Nitzan A and Ratner M A 2003 *Science* **300** 1384
[42] Bastard G 1981 *Phys. Rev.* B **24** 5693
[43] Moth-Poulsen K and Bjørnholm T 2009 *Nat. Nanotechnol.* **4** 551
[44] Landauer R 1957 *IBM J. Res. Dev.* **1** 223
[45] Tao N J 2006 *Nat. Nanotechnol.* **1** 173
[46] Lindsay S M and Ratner M A 2007 *Adv. Mater.* **19** 23
[47] Chen F, Hihath J, Huang Z, Li X and Tao N J 2007 *Annu. Rev. Phys. Chem.* **58** 535
[48] Huisman E H, Guédon C M, van Wees B J and van der Molen S J 2009 *Nano Lett.* **9** 3909
[49] Kergueris C, Bourgoin J-P, Palacin S, Esteve D, Urbina C, Magoga M and Joachim C 1999 *Phys. Rev.* B **59** 12505
[50] Niquet Y M, Delerue C, Allan G and Lannoo M 2002 *Phys. Rev.* B **65** 165334
[51] Delerue C and Lannoo M 2004 *Nanostructures; Theory and Modelling* (Berlin: Springer)
[52] Wu S, Nazin G, Chen X, Qiu X and Ho W 2004 *Phys. Rev. Lett.* **93** 236802
[53] Liljeroth P, Jdira L, Overgaag K, Grandidier B, Speller S and Vanmaekelbergh D 2006 *Phys. Chem. Chem. Phys.* **8** 3845
[54] Datta S 2004 *Nanotechnology* **15** S433
[55] Stipe B C, Rezaei M A and Ho W 1998 *Science* **280** 1732
[56] Heinrich A J, Lutz C P, Gupta J A and Eigler D M 2002 *Science* **298** 1381
[57] Wang W, Lee T, Kretzschmar I and Reed M 2004 *Nano Lett.* **4** 643
[58] Kushmerick J G, Lazorcik J, Patterson C H, Shashidhar R, Seferos D S and Bazan G C 2004 *Nano Lett.* **4** 639
[59] Kiguchi M, Tal O, Wohlthat S, Pauly F, Krieger M, Djukic D, Cuevas J C and van Ruitenbeek J M 2008 *Phys. Rev. Lett.* **101** 046801
[60] Tal O, Krieger M, Leerink B and van Ruitenbeek J M 2008 *Phys. Rev. Lett.* **100** 196804
[61] Lorente N, Persson M, Lauhon L J and Ho W 2001 *Phys. Rev. Lett.* **86** 2593
[62] Viljas J K, Cuevas J C, Pauly F and Häfner M 2005 *Phys. Rev.* B **72** 245415
[63] Gagliardi A, Solomon G C, Pecchia A, Frauenheim T, Carlo A D, Hush N S and Reimers J R 2007 *Phys. Rev.* B **75** 174306
[64] Qiu X H, Nazin G V and Ho W 2004 *Phys. Rev. Lett.* **92** 206102
[65] Ogawa N, Mikaelian G and Ho W 2007 *Phys. Rev. Lett.* **98** 166103
[66] Seldenthuis J S, van der Zant H S J, Ratner M A and Thijssen J M 2008 *ACS Nano* **2** 1445
[67] Wingreen N S, Jacobsen K W and Wilkins J W 1989 *Phys. Rev.* B **40** 11834
[68] Sun Z, Swart I, Delerue C, Vanmaekelbergh D and Liljeroth P 2009 *Phys. Rev. Lett.* **102** 196401
[69] Selzer Y and Allara D L 2006 *Annu. Rev. Phys. Chem.* **57** 593
[70] Galperin M, Ratner M A, Nitzan A and Troisi A 2008 *Science* **319** 1056
[71] Akkerman H B and de Boer B 2008 *J. Phys.: Condens. Matter* **20** 013001
[72] Kröger J, Néel N and Limot L 2008 *J. Phys.: Condens. Matter* **20** 223001
[73] Prokopuk N and Son K-A 2008 *J. Phys.: Condens. Matter* **20** 374116
[74] Binnig G, Rohrer H, Gerber C and Weibel E 1982 *Phys. Rev. Lett.* **49** 57

[75] Binnig G and Rohrer H 1987 *Rev. Mod. Phys.* **59** 615
[76] Nazin G, Qiu X and Ho W 2003 *Science* **302** 77
[77] Lu X, Grobis M, Khoo K, Louie S and Crommie M 2003 *Phys. Rev. Lett.* **90** 096802
[78] Repp J, Meyer G, Stojkovic S M, Gourdon A and Joachim C 2005 *Phys. Rev. Lett.* **94** 026803
[79] Moore A M and Weiss P S 2008 *Annu. Rev. Anal. Chem.* **1** 857
[80] Zandvliet H J W and van Houselt A 2009 *Annu. Rev. Anal. Chem.* **2** 37
[81] Crommie M F, Lutz C P and Eigler D M 1993 *Nature* **363** 524
[82] Manoharan H C, Lutz C P and Eigler D M 2000 *Nature* **403** 512
[83] Tersoff J and Hamann D R 1985 *Phys. Rev.* B **31** 805
[84] Selloni A, Carnevali P, Tosatti E and Chen C D 1985 *Phys. Rev.* B **31** 2602
[85] Lang N D 1986 *Phys. Rev.* B **34** 5947
[86] Hamers R J 1989 *Annu. Rev. Phys. Chem.* **40** 531
[87] Hofer W A, Foster A S and Shluger A L. 2003 *Rev. Mod. Phys.* **75** 1287
[88] Simic-Milosevic V, Mehlhorn M, Rieder K-H, Meyer J and Morgenstern K 2007 *Phys. Rev. Lett.* **98** 116102
[89] Qiu X, Nazin G and Ho W 2003 *Science* **299** 542
[90] Repp J and Meyer G 2006 *Appl. Phys.* A **85** 399
[91] Heinrich A J, Gupta J, Lutz C and Eigler D 2004 *Science* **306** 466
[92] Hirjibehedin C, Lutz C and Heinrich A J 2006 *Science* **312** 1021
[93] Repp J, Meyer G, Paavilainen S, Olsson F E and Persson M 2006 *Science* **312** 1196
[94] Poirier G E 1997 *Chem. Rev.* **97** 1117
[95] Schönenberger C, Jorritsma J, Sondag-Huethorst J A M and Fokkink L G J 1995 *J. Phys. Chem.* **99** 3259
[96] Love J C, Estroff L A, Kriebel J K, Nuzzo R G and Whitesides G M 2005 *Chem. Rev.* **105** 1103
[97] Bumm L A, Arnold J J, Cygan M T, Dunbar T D, Burgin T P, Jones L, Allara D L, Tour J M and Weiss P S 1996 *Science* **271** 1705
[98] Moth-Poulsen K, Patrone L, Stuhr-Hansen N, Christensen J B, Bourgoin J-P and Bjørnholm T 2005 *Nano Lett.* **5** 783
[99] Donhauser Z J *et al* 2001 *Science* **292** 2303
[100] Lewis P A, Inman C E, Yao Y X, Tour J M, Hutchison J E and Weiss P S 2004 *J. Am. Chem. Soc.* **126** 12214
[101] Ramachandran G K, Hopson T J, Rawlett A M, Nagahara L A, Primak A and Lindsay S M 2003 *Science* **300** 1413
[102] Wassel R A, Fuierer R R, Kim N and Gorman C B 2003 *Nano Lett.* **3** 1617
[103] Yasuda S, Nakamura T, Matsumoto M and Shigekawa H 2003 *J. Am. Chem. Soc.* **125** 16430
[104] van der Molen S J, van der Vegte H, Kudernac T, Amin I, Feringa B L and van Wees B J 2006 *Nanotechnology* **17** 310
[105] Katsonis N, Kudernac T, Walko M, van der Molen S J, van Wees B J and Feringa B L 2006 *Adv. Mater.* **18** 1397
[106] Battaglini N, Klein H, Hortholary C, Coudret C, Maurel F and Dumas P 2007 *Ultramicroscopy* **107** 958
[107] Moreland J and Ekin J W 1985 *J. Appl. Phys.* **58** 3888
[108] Muller C J, van Ruitenbeek J M and de Jongh L J 1992 *Physica* C **191** 485
[109] Scheer E, Agraït N, Cuevas J C, Yeyati A L, Ludoph B, Martín-Rodero A, Bollinger G R, van Ruitenbeek J M and Urbina C 1998 *Nature* **394** 154
[110] Grüter L, González M T, Huber R, Calame M and Schönenberger C 2005 *Small* **1** 1067
[111] Vrouwe S A G, van der Giessen E, van der Molen S J, Dulić D, Trouwborst M L and van Wees B J 2005 *Phys. Rev.* B **71** 035313
[112] Trouwborst M L, Huisman E H, Bakker F L, van der Molen S J and van Wees B J 2008 *Phys. Rev. Lett.* **100** 175502
[113] Rubio-Bollinger G, Joyez P and Agraït N 2004 *Phys. Rev. Lett.* **93** 116803
[114] Untiedt C, Caturla M J, Calvo M R, Palacios J J, Segers R C and van Ruitenbeek J M 2007 *Phys. Rev. Lett.* **98** 206801
[115] Reed M A, Zhou C, Muller C J, Burgin T P and Tour J M 1997 *Science* **278** 252
[116] Reichert J, Ochs R, Beckmann D, Weber H B, Mayor M and Löhneysen H v 2002 *Phys. Rev. Lett.* **88** 176804
[117] Dulić D, van der Molen S J, Kudernac T, Jonkman H T, de Jong J J D, Bowden T N, van Esch J, Feringa B L and van Wees B J 2003 *Phys. Rev. Lett.* **91** 207402
[118] Lörtscher E, Ciszek J W, Tour J and Riel H 2006 *Small* **2** 973
[119] Böhler T, Edtbauer A and Scheer E 2007 *Phys. Rev.* B **76** 125432
[120] Suzuki M, Fujii S and Fujihira M 2006 *Japan. J. Appl. Phys.* **45** 2041
[121] Gonzalez M T, Wu S, Huber R, van der Molen S J, Schönenberger C and Calame M 2006 *Nano Lett.* **6** 2238
[122] Tsutsui M, Shoji K, Morimoto K, Taniguchi M and Kawai T 2008 *Appl. Phys. Lett.* **92** 223110
[123] Tsutsui M, Shoji K, Taniguchi M and Kawai T 2008 *Nano Lett.* **8** 345
[124] Huisman E H, Trouwborst M L, Bakker F L, de Boer B, van Wees B J and van der Molen S J 2008 *Nano Lett.* **8** 3381
[125] Martin C A, Ding D, van der Zant H S J and van Ruitenbeek J M 2008 *New J. Phys.* **10** 065008
[126] Thijssen W H A, Djukic D, Otte A F, Bremmer R H and van Ruitenbeek J M 2006 *Phys. Rev. Lett.* **97** 226806
[127] Tal O, Kiguchi M, Thijssen W H A, Djukic D, Untiedt C, Smit R H M and van Ruitenbeek J M 2009 *Phys. Rev.* B **80** 085427
[128] Xu B and Tao N J 2003 *Science* **301** 1221
[129] Huang J, Li Q, Ren H, Su H, Shi Q W and Yang J 2007 *J. Chem. Phys.* **127** 13225
[130] Xu B Q, Zhang P M, Li X L and Tao N J 2004 *Nano Lett.* **4** 1105
[131] Xu B, Xiao X and Tao N J 2003 *J. Am. Chem. Soc.* **125** 16164
[132] Xia J L, Diez-Perez I and Tao N J 2008 *Nano Lett.* **8** 1960
[133] Hihath J, Arroyo C R, Rubio-Bollinger G, Tao N J and Agraït N 2008 *Nano Lett.* **8** 1673
[134] Li X, He J, Hihath J, Xu B, Lindsay S M and Tao N J 2006 *J. Am. Chem. Soc.* **128** 2135
[135] He J *et al* 2005 *Nanotechnology* **16** 695
[136] Li C, Mishchenko A, Li Z, Pobelov I, Wandlowski T, Li X Q, Wrthner F, Bagrets A and Evers F 2008 *J. Phys.: Condens. Matter* **20** 374122
[137] Mészáros G, Li C, Pobelov I and Wandlowski T 2007 *Nanotechnology* **18** 424004
[138] Venkataraman L, Klare J E, Tam I W, Nuckolls C, Hybertsen M S and Steigerwald M L 2006 *Nano Lett.* **6** 458
[139] Hybertsen M S, Venkataraman L, Klare J E, Whalley A C, Steigerwald M L and Nuckolls C 2008 *J. Phys.: Condens. Matter* **20** 374115
[140] Haiss W, Nichols R J, van Zalinge H, Higgins S J, Bethell D and Schiffrin D J 2004 *Phys. Chem. Chem. Phys.* **6** 4330
[141] Haiss W, van Zalinge H, Bethell D, Ulstrup J, Schiffrin D J and Nichols R J 2006 *Faraday Discuss.* **131** 253
[142] Kockmann D, Poelsema B and Zandvliet H J W 2009 *Nano Lett.* **9** 1147
[143] Temirov R, Lassise A, Anders F B and Tautz F S 2008 *Nanotechnology* **19** 065401
[144] Lafferentz L, Ample F, Yu H, Hecht S, Joachim C and Grill L 2009 *Science* **323** 1193
[145] Park H, Lim A K L, Alivisatos A P, Park J and McEuen P L 1999 *Appl. Phys. Lett.* **75** 301
[146] Sorbello R 1997 *Solid State Physics* vol 51 (New York: Academic) pp 159–231
[147] van der Molen S J, Welling M S and Griessen R 2000 *Phys. Rev. Lett.* **85** 3882

[148] van der Zant H S J *et al* 2006 *Faraday Discuss.* **131** 347
[149] Park H, Park J, Lim A K L, Anderson E H, Alivisatos A P and McEuen P L 2000 *Nature* **407** 57
[150] Liang W, Shores M P, Bockrath M, Long J R and Park H 2002 *Nature* **417** 725
[151] Park J *et al* 2002 *Nature* **417** 722
[152] Lambert M F, Goffman M F and Hesto J P B P 2003 *Nanotechnology* **14** 772
[153] Trouwborst M L, van der Molen S J and van Wees B J 2006 *J. Appl. Phys.* **99** 114316
[154] Wu Z M, Steinacher M, Huber R, Calame M, van der Molen S J and Schönenberger C 2007 *Appl. Phys. Lett.* **91** 053118
[155] Houck A A, Labaziewicz J, Chan E K, Folk J A and Chuang I L 2005 *Nano Lett.* **5** 1685
[156] Heersche H B, de Groot Z, Folk J A, Kouwenhoven L P, van der Zant H S J, Houck A A, Labaziewicz J and Chuang I L 2006 *Phys. Rev. Lett.* **96** 017205
[157] Esen G and Fuhrer M S 2005 *Appl. Phys. Lett.* **87** 263101
[158] Strachan D R, Smith D E, Johnston D E, Park T-H, Therien M J, Bonnell D A and Johnson A T 2005 *Appl. Phys. Lett.* **86** 043109
[159] Taychatanapat T, Bolotin K I, Kuemmeth F and Ralph D C 2007 *Nano Lett.* **7** 652
[160] Morpurgo A F, Marcus C M and Robinson D B 1999 *Appl. Phys. Lett.* **74** 2084
[161] Kervennic Y-V, Thijssen J M, Vanmaekelbergh D, Dabirian R, Jenneskens L W, van Walree C A and van der Zant H S J 2006 *Angew. Chem. Int. Edn* **45** 2540
[162] Kubatkin S, Danilov A, Hjort M, Cornil J, Brédas J-L, Stuhr-Hansen N, Hedegård P and Bjørnholm T 2003 *Nature* **425** 698
[163] Guo X *et al* 2006 *Science* **311** 356
[164] Whalley A C, Steigerwald M L, Guo X and Nuckolls C 2007 *J. Am. Chem. Soc.* **129** 12590
[165] Long D P, Patterson C H, Moore M H, Seferos D S, Bazan G C and Kushmerick J G 2005 *Appl. Phys. Lett.* **86** 153105
[166] Andres R P, Bielefeld J D, Henderson J I, Janes D B, Kolagunta V R, Kubiak C P, Mahoney W J and Osifchin R G 1996 *Science* **273** 1690
[167] Dadosh T, Gordin Y, Krahne R, Khivrich I, Mahalu D, Frydman V, Sperling J, Yacoby A and Bar-Joseph I 2005 *Nature* **436** 677
[168] Bernard L, Calame M, van der Molen S J, Liao J and Schönenberger C 2007 *Nanotechnology* **18** 235202
[169] Hassenkam T, Moth-Poulsen K, Stuhr-Hansen N, Norgaard K, Kabir M S and Bjørnholm T 2004 *Nano Lett.* **4** 19
[170] Xu C *et al* 2006 *Nanotechnology* **17** 3333
[171] Liao J, Bernard L, Langer M, Schönenberger C and Calame M 2006 *Adv. Mater.* **18** 2444
[172] Bernard L, Kamdzhilov Y, Calame M, van der Molen S J, Liao J and Schönenberger C 2007 *J. Phys. Chem.* C **111** 18445
[173] Robinson D B, Funamura J R, Talin A A and Anderson R J 2007 *Appl. Phys. Lett.* **90** 083119
[174] Ikeda M, Tanifuji N, Yamaguchi H, Irie M and Matsuda K 2007 *Chem. Commun.* 1355–7
[175] Matsuda K, Yamaguchi H, Sakano T, Ikeda M, Tanifuji N and Irie M 2008 *J. Phys. Chem.* C **112** 17005
[176] Liao J, Mangold M A, Grunder S, Mayor M, Schönenberger C and Calame M 2008 *New J. Phys.* **10** 065019
[177] van der Molen S J, Liao J, Kudernac T, Agustsson J S, Bernard L, Calame M, van Wees B J, Feringa B L and Schönenberger C 2009 *Nano Lett.* **9** 76
[178] Brust M, Schiffrin D J, Bethell D and Kiely C J 1995 *Adv. Mater.* **7** 795
[179] Xia Y and Whitesides G M 1998 *Angew. Chem. Int. Edn* **37** 550
[180] Loo Y-L, Lang D V, Rogers J A and Hsu J W P 2003 *Nano Lett.* **3** 913
[181] Slowinski K, Chamberlain R V, Miller C J and Majda M 1997 *J. Am. Chem. Soc.* **119** 11910
[182] Rampi M A, Schueller O J A and Whitesides G M 1998 *Appl. Phys. Lett.* **72** 1781
[183] Haag R, Rampi M A, Holmlin R E and Whitesides G M 1999 *J. Am. Chem. Soc.* **121** 7895
[184] Tran E, Duati M, Ferri V, Müllen K, Zharnikov M, Whitesides G M and Rampi M A 2006 *Adv. Mater.* **18** 1323
[185] Kushmerick J G, Holt D B, Yang J C, Naciri J, Moore M H and Shashidhar R 2002 *Phys. Rev. Lett.* **89** 086802
[186] Kushmerick J G, Holt D B, Pollack S K, Ratner M A, Yang J C, Schull T L, Naciri J, Moore M H and Shashidhar R 2002 *J. Am. Chem. Soc.* **124** 10654
[187] Collier C P, Wong E W, Belohradský M, Raymo F M, Stoddart J F, Kuekes P J, Williams R S and Heath J R 1999 *Science* **285** 391
[188] Luo Y *et al* 2002 *ChemPhysChem* **3** 519
[189] Green J E *et al* 2007 *Nature* **445** 414
[190] Akkerman H B, Blom P W M, de Leeuw D M and de Boer B 2006 *Nature* **441** 69
[191] Kronemeijer A J, Akkerman H B, Kudernac T, van Wees B J, Feringa B L, Blom P W M and de Boer B 2008 *Adv. Mater.* **20** 1467
[192] Milani F, Grave C, Ferri V, Samori P and Rampi M A 2007 *ChemPhysChem* **8** 515
[193] Eigler D M and Schweizer E K 1990 *Nature* **344** 524
[194] Stroscio J A and Eigler D M 1991 *Science* **254** 1319
[195] Moresco F, Meyer G, Rieder K-H, Tang H, Gourdon A and Joachim C 2001 *Phys. Rev. Lett.* **86** 672
[196] Chen J, Reed M A, Rawlett A M and Tour J M 1999 *Science* **286** 1550
[197] Lewis P A, Inman C E, Maya F, Tour J M, Hutchison J E and Weiss P S 2005 *J. Am. Chem. Soc.* **127** 17421
[198] Moore A M, Dameron A A, Mantooth B A, Smith R K, Fuchs D J, Ciszek J W, Maya F, Yao Y X, Tour J M and Weiss P S 2006 *J. Am. Chem. Soc.* **128** 1959
[199] Moore A M, Mantooth B A, Donhauser Z J, Yao Y X, Tour J M and Weiss P S 2007 *J. Am. Chem. Soc.* **129** 10352
[200] Hallback A-S, Poelsema B and Zandvliet H J W 2007 *ChemPhysChem* **8** 661
[201] Blum A S, Kushmerick J G, Long D P, Patterson C H, Yang J C, Henderson J C, Yao Y, Tour J M, Shashidhar R and Ratna B R 2005 *Nat. Mater.* **4** 167
[202] Quek S Y, Kamenetska M, Steigerwald M L, Choi H J, Louie S G, Hybertsen M S, Neaton J B and Venkataraman L 2009 *Nat. Nanotechnol.* **4** 230
[203] Trouwborst M L, Huisman E H, van der Molen S J and van Wees B J 2009 *Phys. Rev.* B **80** 081407
[204] Halbritter A, Makk P, Csonka S and Mihaly G 2008 *Phys. Rev.* B **77** 075402
[205] Danilov A V, Hedegård P, Golubev D S, Bjørnholm T and Kubatkin S E. 2008 *Nano Lett.* **8** 2393
[206] Risse T, Shaikhutdinov S, Nilius N, Sterrer M and Freund H-J 2008 *Acc. Chem. Res.* **41** 949
[207] Seo K, Konchenko A V, Lee J, Bang G S and Lee H 2008 *J. Am. Chem. Soc.* **130** 2553
[208] Gittins D I, Bethell D, Schiffrin D J and Nichols R J 2000 *Nature* **408** 67
[209] Xiao X Y, Nagahara L A, Rawlett A M and Tao N J 2005 *J. Am. Chem. Soc.* **127** 9235
[210] Xu B Q, Xiao X Y, Yang X M, Zang L and Tao N J 2005 *J. Am. Chem. Soc.* **127** 2386
[211] Haiss W *et al* 2007 *J. Phys. Chem.* B **111** 6703
[212] Albrecht T, Moth-Poulsen K, Christensen J B, Hjelm J, Bjørnholm T and Ulstrup J 2006 *J. Am. Chem. Soc.* **128** 6574
[213] Leary E, Higgins S J, van Zalinge H, Haiss W, Nichols R J, Nygaard S, Jeppesen J O and Ulstrup J 2008 *J. Am. Chem. Soc.* **130** 12204

[214] Li Z, Pobelov I, Han B, Wandlowski T, Blaszczyk A and Mayor M 2007 *Nanotechnology* **18** 044018
[215] Pobelov I V, Li Z and Wandlowski T 2008 *J. Am. Chem. Soc.* **130** 16045
[216] Tsoi S, Griva I, Trammell S A, Blum A S, Schnur J M and Lebedev N 2008 *ACS Nano* **2** 1289
[217] van Dijk E H, Myles D J T, van der Veen M H and Hummelen J C 2006 *Org. Lett.* **8** 2333
[218] Liao J *et al* 2010 Cyclic conductance switching in networks of redox-active molecular junctions *Nano. Lett.* **10** 759–64
[219] Deng W-Q, Muller R P and Goddard W A 2004 *J. Am. Chem. Soc.* **126** 13562
[220] Collier C P, Mattersteig G, Wong E W, Luo Y, Beverly K, Sampaio J, Raymo F M, Stoddart J F and Heath J R 2000 *Science* **289** 1172
[221] Collier C P, Jeppesen J O, Luo Y, Perkins J, Wong E W, Heath J R and Stoddart J F 2001 *J. Am. Chem. Soc.* **123** 12632
[222] Diehl M R, Steuerman D W, Tseng H-R, Vignon S A, Star A, Celestre P C, Stoddart J F and Heath J R 2003 *ChemPhysChem* **4** 1335
[223] Chen Y, Ohlberg D A A, Li X, Stewart D R, Williams R S, Jeppesen J O, Nielsen K A, Stoddart J F, Olynick D L and Anderson E 2003 *Appl. Phys. Lett.* **82** 1610
[224] Service R F 2003 *Science* **302** 556
See also the replies by Heath, Stoddart and Williams 2004 *Science* **303** 1136
[225] Lau C N, Stewart D R, Williams R S and Bockrath M 2004 *Nano Lett.* **4** 569
[226] Blackstock J J, Donley C L, Stickle W F, Ohlberg D A A, Yang J J, Stewart D R and Williams R S 2008 *J. Am. Chem. Soc.* **130** 4041
[227] Flood A H, Stoddart J F, Steuerman D W and Heath J R 2004 *Science* **306** 2055
[228] Flood A H, Peters A J, Vignon S A, Steuerman D W, Tseng H R, Kang S, Heath J R and Stoddart J F 2004 *Chem. Eur. J.* **10** 6558
[229] Flood A H, Wong E W and Stoddart J F 2006 *Chem. Phys.* **324** 280
[230] Choi J *et al* 2006 *Chem. Eur. J.* **12** 261
[231] Katz E, Baron R, Willner I, Richke N and Levine R D 2005 *ChemPhysChem* **6** 2179
[232] DeIonno E, Tseng H-R, Harvey D D, Stoddart J F and Heath J R 2006 *J. Phys. Chem.* B **110** 7609
[233] Waldeck D 1991 *Chem. Rev.* **91** 415
[234] Browne W R, Kudernac T, Katsonis N, Areephong J, Hielm J and Feringa B L 2008 *J. Phys. Chem.* C **112** 1183
[235] Kudernac T, Katsonis N, Browne W R and Feringa B L 2009 *J. Mater. Chem.* **19** 7168
[236] del Valle M, Gutiérrez R, Tejedor C and Cuniberti G 2007 *Nat. Nanotechnol.* **2** 176
[237] Wolf M and Tegeder P 2009 *Surf. Sci.* **603** 1506
[238] Benesch C, Rode M F, Cizek M, Haertle R, Rubio-Pons O, Thoss M and Sobolewski A L 2009 *J. Phys. Chem.* C **113** 10315
[239] Zhao P, Fang C F, Wang Y M, Zhai Y X and Liu D S 2009 *Physica* E **41** 474
[240] Dri C, Peters M V, Schwarz J, Hecht S and Grill L 2008 *Nat. Nanotechnol.* **3** 649
[241] Kumar A S, Ye T, Takami T, Yu B-C, Flatt A K, Tour J M and Weiss P S 2008 *Nano Lett.* **8** 1644
[242] Zhao P, Wang P, Zhang Z, Fang C, Wang Y, Zhai Y and Liu D 2009 *Solid State Commun.* **149** 928
[243] Mativetsky J M, Pace G, Elbing M, Rampi M A, Mayor M and Samori P 2008 *J. Am. Chem. Soc.* **130** 9192
[244] Ferri V, Elbing M, Pace G, Dickey M D, Zharnikov M, Samori P, Mayor M and Rampi M A 2008 *Angew. Chem. Int. Edn* **47** 3407
[245] Kelly T, De Silva H and Silva R 1999 *Nature* **401** 150
[246] Koumura N, Zijlstra R W J, van Delden R A, Harada N and Feringa B L 1999 *Nature* **401** 152
[247] Leigh D A, Wong J K Y, Dehez F and Zerbetto F 2003 *Nature* **424** 174
[248] Berna J, Leigh D A, Lubomska M, Mendoza S M, Perez E M, Rudolf P, Teobaldi G and Zerbetto F 2005 *Nat. Mater.* **4** 704
[249] Browne W R and Feringa B L 2006 *Nat. Nanotechnol.* **1** 25
[250] Geertsema E M, van der Molen S J, Martens M and Feringa B L 2009 *Proc. Natl Acad. Sci. USA* **106** 16919
[251] Kudernac T, van der Molen S J, van Wees B J and Feringa B L 2006 *Chem. Commun.* 3597–9
[252] Matsuda K and Irie M 2000 *J. Am. Chem. Soc.* **122** 7195
[253] Fraysse S, Coudret C and Launay J-P 2000 *Eur. J. Inorg. Chem.* 1581
[254] Irie M, Fukaminato T, Sasaki T, Tamai N and Kawai T 2002 *Nature* **420** 759
[255] Okabe C, Tanaka N, Fukaminato T, Kawai T, Irie M, Nibu Y, Shimada H, Goldberg A, Nakamura S and Sekiya H 2002 *Chem. Phys. Lett.* **357** 113
[256] Tsujioka T and Kondo H 2003 *Appl. Phys. Lett.* **83** 937
[257] Hania R, Pugẑlys A, Kudernac T, Jonkman H and Duppen K 2005 *Springer Ser. Chem. Phys.* **79** 679
[258] Li J, Speyer G and Sankey O F 2004 *Phys. Rev. Lett.* **93** 248302
[259] Zhuang M and Ernzerhof M 2005 *Phys. Rev.* B **72** 073104
[260] Kondo M, Tada T and Yoshizawa K 2005 *Chem. Phys. Lett.* **412** 55
[261] Perrier A, Maurel F and Aubard J 2007 *J. Phys. Chem.* A **111** 9688
[262] Sauer P and Allen R E 2007 *Chem. Phys. Lett.* **434** 260
[263] Staykov A, Nozaki D and Yoshizawa K 2007 *J. Phys. Chem.* C **111** 3517
[264] Huang Z F, Chen F, Bennett P A and Tao N J 2007 *J. Am. Chem. Soc.* **129** 13225
[265] Zhuang M and Ernzerhof M 2009 *J. Chem. Phys.* **130** 114704
[266] Kudernac T, de Jong J J, van Esch J, Feringa B L, Dulić D, van der Molen S J and van Wees B J 2005 *Mol. Cryst. Liq. Cryst.* **430** 205
[267] Mayor M, Weber H, Reichert J, Elbing M, von Hänisch C, Beckmann D and Fischer M 2003 *Angew. Chem. Int. Edn* **42** 5834
[268] Rampi M A, private communication
[269] Gross L, Mohn F, Liljeroth P, Repp J, Giessibl F J and Meyer G 2009 *Science* **324** 1428
[270] Gross L, Mohn F, Moll N, Liljeroth P and Meyer G 2009 *Science* **325** 1110
[271] Osorio E A, Ruben M, Seldenthuis J S, Lehn J-M and van der Zant H S J 2010 *Small* **6** 174